NASA TECHNICAL MEMORANDUM

NASA TM X- 62,418

NASA TM X- 62,418

(NASA-TM-X-62418) SHAKE TEST OF ROTOR TEST APPARATUS IN THE 40- BY 80-FOOT WIND TUNNEL (NASA) 74 p HC $4.25 CSCL 14B

N75-20350

Unclas
G3/09 14696

SHAKE TEST OF ROTOR TEST APPARATUS IN THE 40- BY 80-FOOT WIND TUNNEL

Wayne Johnson and James C. Biggers

Ames Research Center
and
U. S. Army Air Mobility R&D Laboratory
Moffett Field, Calif. 94035

February 1975

1. Report No.	2. Government Accession No.	3. Recipient's Catalog No.
TM X 62,418		

4. Title and Subtitle	5. Report Date
SHAKE TEST OF ROTOR TEST APPARATUS IN THE 40- BY 80-FOOT WIND TUNNEL	
	6. Performing Organization Code

7. Author(s)	8. Performing Organization Report No.
Wayne Johnson and James C. Biggers	A-5973
	10. Work Unit No.
9. Performing Organization Name and Address	505-10-21
Ames Research Center and U. S. Army Air Mobility R&D Laboratory Moffett Field, Calif. 94035	11. Contract or Grant No.

12. Sponsoring Agency Name and Address	13. Type of Report and Period Covered
National Aeronautics and Space Administration Washington, D. C. 20546	Technical Memorandum
	14. Sponsoring Agency Code

15. Supplementary Notes

16. Abstract

A shake test was conducted to determine the dynamic characteristics of a Rotor Test Apparatus on two strut systems in the Ames 40- by 80-ft wind tunnel. The rotor-off hub transfer function (acceleration per unit force as a function of frequency) was measured in the longitudinal and lateral directions, using a combination of broadband and discrete frequency excitation techniques. The dynamic data is summarized for the configurations tested, giving the following properties for each mode identified: the natural frequency, the hub response at resonance, and the fixed system damping. The complete transfer functions are presented, and the detailed test results are included as an appendix. Finally, the report discusses the data analysis techniques developed to obtain on-line measurements of the system modal properties, including the damping coefficient and the damping ratio.

17. Key Words (Suggested by Author(s))	18. Distribution Statement
Rotor test apparatus Shake test Wind tunnel	Unclassified - Unlimited STAR Category - 09

19. Security Classif. (of this report)	20. Security Classif. (of this page)	21. No. of Pages	22. Price*
Unclassified	Unclassified	74	$4.25

*For sale by the National Technical Information Service, Springfield, Virginia 22151

SHAKE TEST OF ROTOR TEST APPARATUS IN THE 40- BY 80-FT WIND TUNNEL

Wayne Johnson* and James C. Biggers**

Ames Research Center
Moffett Field, California

SUMMARY

A shake test was conducted to determine the dynamic characteristics of a Rotor Test Apparatus on two strut systems in the Ames 40- by 80-ft wind tunnel. The rotor-off hub transfer function (acceleration per unit force as a function of frequency) was measured in the longitudinal and lateral directions, using a combination of broadband and discrete frequency excitation techniques. The dynamic data is summarized for the configurations tested, giving the following properties for each mode identified: the natural frequency, the hub response at resonance, and the fixed system damping. The complete transfer functions are presented, and the detailed test results are included as an appendix. Finally, the report discusses the data analysis techniques developed to obtain on-line measurements of the system modal properties, including the damping coefficient and the damping ratio.

INTRODUCTION

A shake test was conducted to establish the dynamic characteristics of a Rotor Test Apparatus (RTA) in the Ames 40- by 80-ft wind tunnel (figure 1). Of interest were potential resonances at the 1/rev and 4/rev frequencies of rotors likely to be tested on the RTA, and potential ground resonance instabilities.

The shake test was performed on the RTA module, without a rotor, on two strut systems in the wind tunnel, to determine the principle frequencies and damping of the structure. The rotor-off hub transfer function was

*Research Scientist, U.S. Army Air Mobility Research and Development Laboratory

**Research Scientist, National Aeronautics and Space Administration

measured in the longitudinal and lateral directions: longitudinal, inplane acceleration of the hub due to longitudinal, inplane force; and lateral, inplane acceleration of the hub due to lateral, inplane force. With the hub transfer functions it is possible to evaluate potential ground resonance and vibration problems of rotors to be tested on the RTA. The frequency ranges of interest are: 0-5 Hz for ground resonance, 3-7.5 Hz for 1/rev vibration, and 12-30 Hz for 4/rev vibration (based on a rotor speed range of 180-450 rpm). The information required for each mode of the system is the natural frequency and the amplitude of the hub response, and for potential ground resonance modes we must know the fixed system damping as well.

SYSTEM

The system tested consisted of the RTA module, without a rotor, on the struts and balance frame in the 40- by 80-ft wind tunnel. The RTA module included the rotor hub, with the transmission locked, and two 1500-HP electric motors installed (one of the motors was replaced by a dummy weight for this test). The total module weight was 30400 lb.

Two strut/tip configurations were tested: a short strut system (8-ft struts with 5-ft tips) and a long strut system (15-ft struts with 6-in tips). The short struts gave softer support of the module because of the flexibility of the tips. In the basic configuration the balance was free, with the scale system operating. The shake tests were also conducted with the balance locked, in order to obtain the cantilever strut modes. Finally, the system was tested with strut dampers installed, consisting of an extensible strut from the top of each main strut down to the rear of the balance frame, with a total of eight automotive shock absorbers as dampers.

TEST APPARATUS

A hydraulic shaker was attached to the blade grip of the rotor hub to excite the module by application of an inplane force, in the longitudinal or lateral direction. The other end of the shaker was attached to an

11600 lb reaction mass suspended from a crane. Figure 2 shows the shake test configuration, for lateral excitation. For longitudinal excitation, the shaker was attached to the forward blade grip, with the reaction mass over the module nose. The shaker servo control was operated in a stroke feedback mode.

A load cell between the shaker and hub measured the applied force. Accelerometers on the hub measured the longitudinal and lateral response. Data were recorded for other accelerometers on the module and balance frame, but only the results for the hub response are presented in this report.

The applied force and resulting hub acceleration data were analyzed on-line to determine the dynamic characteristics of the system, using the Dynamic Analysis System (DAS, shown in figure 3). The DAS is basically a time series analyzer and computer, utilizing Fast Fourier Transform techniques and associated software, and programs specific to this shake test.

TEST PROCEDURE

The frequency ranges investigated were 0-9 Hz for ground resonance and 1/rev vibration modes, and 0-35 Hz for N/rev vibration modes. Broadband random input to the shaker was used, with a bandpass filter to shape the input spectrum. The low cutoff frequency was set at 0.5 Hz to avoid excitation of the reaction mass pendulum modes, and the high cutoff frequency was set at either 9 or 35 Hz to restrict the energy input to the frequency range of interest.

The basic test plan, for each strut/module/balance configuration, excited in the longitudinal and lateral directions, was as follows.

1) Random excitation, bandwidth .5-9 Hz; nominal force amplitude ±200 and ±400 lb (±400 lb point usually repeated).
2) Random excitation, bandwidth .5-35 Hz; nominal force amplitude ±100 and ±200 lb.

3) Sinusoidal (discrete frequency) excitation at various force levels, at the low frequency resonances identified in #1; usually points were taken at frequencies near the resonance as well.

There was some variation between runs of course. For future work, the use of narrow-band random excitation at each resonance would seem preferable to a sequence of (nominally) discrete frequency points as was the practice in this test. Narrow-band excitation offers the possibility of obtaining the data over the entire frequency range near the resonance in a single measurement. The reason for the narrow-band excitation is to concentrate the input energy into a particular mode, so for the highest force levels it may be necessary to narrow it down to essentially discrete excitation again. Still, the data from this test indicate that an accurate estimate of the system damping may be obtained from the single frequency point, even if it is not quite at the resonant peak (see the discussions below).

The following six configurations were tested, with longitudinal and lateral excitation for each:

1) Short struts.
2) Short struts, balance locked.
3) Short struts, with strut dampers (8 shocks).
4) Long struts.
5) Long struts, balance locked.
6) Long struts, with strut dampers (8 shocks).

ANALYSIS

The data for the force applied to the hub and the resulting hub acceleration were analyzed on-line, utilyzing the DAS. The input signal f (force) and output signal a (acceleration) were sampled (digitized) at rate r, taking a total of N samples. The discrete Fourier transforms of f and a were calculated, and converted to engineering units using input conversion factors (lb/volt and g/volt). The products of the transforms gave the cross spectrum $S_{io} = \overline{F}*A$, and the input autospectrum $S_{ii} = \overline{F}*F$. S_{io} and S_{ii} were averaged over K data records. Finally the transfer function of the hub response was calculated, from H = acceleration/force = averaged S_{io}/averaged S_{ii}.

The computer searched the magnitude of the transfer function for resonant peaks. Then it calculated and printed for each peak the following quantities: the resonant frequency ω (Hz); the magnitude of the force and acceleration at that frequency; the magnitude of the hub response $|H|$ (g/1000 lb and in/1000 lb); the phase of the response, $\angle H$ (deg); the fixed system damping coefficient C_s (lb/fps), calculated from H at the resonant frequency; the damping coefficient, modal mass, and damping ratio (C_s, M, and ζ), calculated from integrals of H through the resonant peak; and the damping ratio ζ , calculated by a least-squared-error parameter identification technique from the data for H near the peak. In addition, ground resonance parameters (critical rotor speed and required lag damping) were calculated, for a particular rotor.

The magnitude of the transfer function, $|H|$ vs. ω , was displayed on a CRT. A picture was taken as a record of the complete transfer function.

The discrete frequency excitation points were analyzed in the same manner. However, the response was only evaluated at the single line corresponding to the input frequency.

Further details of the analysis techniques are given in appendices: a discussion of the discrete Fourier transform (Appendix A); the local maximum discriminator (Appendix B); calculation of the fixed system damping from the transfer function (Appendix C); LSE parameter identification of the damping ratio (Appendix D); and calculation of the damping from integrals of the transfer function (Appendix E).

The following parameters were used for the analysis of the data in this test:

1) Ground resonance and 1/rev dynamics (0-9 Hz): sample rate r = 20.48/sec, number of samples N = 512, number of records K = 10; total sample time T = 250 sec, spectrum frequency increment $\Delta\omega$ = .04 Hz.

2) N/rev dynamics (0-35 Hz): sample rate $r = 81.92$/sec, number of samples $N = 256$, number of records $K = 20$; total sample time $T = 62.5$ sec, and spectrum frequency increment $\Delta\omega = .32$ Hz.

For future work, it would probably be better to take more records for the 35 Hz bandwidth excitation, to further reduce the noise in the data; $K = 40$ (hence $T = 125$ sec) should be about right. The use of Hanning to smooth the data is usually recommended (see the references of Appendix A), but it was only occasionally used in this test.

RESULTS

The results of this test are the dynamic characteristics of the six configurations investigated, specifically, the frequencies and response amplitudes of the principal modes identifiable in the hub transfer functions.

Figure 4 demonstrates the repeatibility of the transfer function measurements. It shows three separate measurements of the longitudinal response on the short struts. There is excellent correlation between the three points. Figures 5 through 10 present the transfer functions for the six configurations tested. The lateral and longitudinal hub responses are shown, in the 9 and 35 Hz excitation ranges for each. The abscissas in the figures are frequency, from 0 to 10 or 50 Hz, and the ordinates are the magnitude of the transfer function in g/1000 lb.

Tables 1 and 2 summarize the dynamic characteristics of the six configurations tested. The tables give the following quantities for each of the longitudinal and lateral modes identified: the resonant frequency ω (Hz); the magnitude of the hub response H (g/1000 lb and in/1000 lb); and, for the potential ground resonance modes, the fixed system damping coefficient C_s (lb/fps). The hub response and damping coefficient data for the long struts, lateral shake, balance free and balance locked (runs 17 and 18) are somewhat uncertain because of a problem with the accelerometer calibration. However, the conversion factor (g/volt) used for these two runs was certainly within 25% of the correct factor. The frequency and damping ratio data are nof affected by this problem.

TABLE 1. Summary of Dynamic Characteristics: Short Struts

Longitudinal Modes: Mode		ω Hz	H g/1000 lb	H in/1000 lb	C_s lb/fps		Lateral Modes: Mode		ω Hz	H g/1000 lb	H in/1000 lb	C_s lb/fps
SHORT STRUTS												
balance		1.66	.21	.39	1300-1500		balance	side	2.10	.36	.80	1000-1100
strut		3.04	.38	.40	800-1200		balance	yaw	2.24	.34	.67	500-600
balance	vertical	7.32	.15	.03			strut		3.52	.41	.32	1400-1600
module	vertical	10.0	.90	.09			mast		23.2	2.9	.05	
X-beam	vertical	14.1	.70	.03			mast		27.7	2.3	.03	
mast		25.5	3.1	.05								
		28.5	1.5	.02								
		31.2	1.7	.02								
		35.0	2.0	.02								
SHORT STRUTS, BALANCE LOCKED												
strut		2.27	.78	1.47	440		strut		2.45	1.40	2.28	300
module	vertical	10.0	.80	.08			mast		23.7	2.0	.03	
X-beam	vertical	15.3	.50	.02			mast		27.7	1.9	.02	
mast		25.5	2.5	.04								
		31.2	1.3	.01								
		35.0	1.5	.01								
SHORT STRUTS, WITH STRUT DAMPERS												
balance		1.70	.09	.30	3200-3600		balance	side	1.9	.20	.50	1800-2000
damper	strut	4.9	.15	.06	4000-6000		balance	yaw	2.2	.20	.42	1900-2100
strut		5.8	.12	.04	4000-8000		strut		3.52	.22	.18	2900-3200
balance	vertical	7.60	.09	.01			mast		23.2	3.5	.06	
module	vertical	10.7	.80	.07			mast		27.7	3.3	.04	
X-beam	vertical	15.5	.55	.02								
mast		25.5	3.2	.05								
		28.5	1.5	.02								
		31.2	1.7	.02								
		35.0	2.0	.02								

TABLE 2. Summary of Dynamic Characteristics: Long Struts

Longitudinal Modes							Lateral Modes					
Mode		ω Hz	H g/ 1000 lb	H in/ 1000 lb	C_s lb/fps		Mode		ω Hz	H g/ 1000 lb	H in/ 1000 lb	C_s lb/fps
					LONG STRUTS							
balance		1.62	.09	.32	3400-3800		balance	side	2.32	.21	.38	1600-2000
strut		4.02	.85	.51	600-800		balance	yaw	2.67	.18	.25	2600-3000
balance	vertical	7.20	.09	.02			strut		4.50	1.24	.60	550-650
module	vertical	10.6	.70	.06			mast		23.2	1.0	.02	
X-beam	vertical	14.1	.65	.03			mast		27.7	2.5	.03	
mast		25.5	2.5	.04								
		28.5	1.6	.02								
		31.2	1.4	.01								
		35.0	1.5	.01								
					LONG STRUTS, BALANCE LOCKED							
strut		3.00	1.15	1.25	500		strut		3.46	1.55	1.27	280
module	vertical	10.2	.85	.08			mast		23.2	1.5	.03	
X-beam	vertical	15.2	.60	.03			mast		27.7	2.2	.03	
mast		25.5	2.1	.03								
		31.2	1.2	.01								
		35.0	1.4	.01								
					LONG STRUTS WITH STRUT DAMPERS							
balance		1.61	.07	.26	3600-4200		balance	side	2.32	.24	.44	1400-1800
damper	strut	3.61	.10	.07	5000-6400		balance	yaw	3.2	.02	.02	
strut		5.48	.31	.10	3200-4600		strut		4.65	.31	.14	2800-3000
balance	vertical	7.38	.07	.01			mast		23.2	2.0	.04	
module	vertical	10.7	.80	.07			mast		27.7	2.6	.03	
X-beam	vertical	15.5	.65	.03								
mast		25.5	2.5	.04								
		28.5	1.4	.02								
		31.2	1.4	.01								
		35.0	1.4	.01								

In the lateral response on the short struts (balance free, no dampers) we observe two close modes at the lower resonance, around 2 Hz. These are the balance side and balance yaw modes, involving considerable module yaw and side motion as well for this case. Figure 11 shows the details of the two modes, expanding the magnitude and phase of the transfer function in the range 1-3 Hz. The detailed test data are given in Appendix G, Table G1. The dynamic situation is as follows. For the short strut configuration, the uncoupled balance lateral modes and cantilever strut side mode have about the same frequency, around 2.4 Hz (see Tables 1 and 2). Thus there is considerable coupling of the balance and module motion for the complete system, with the typical behavior that the frequencies of the coupled modes are driven apart. The balance mode frequencies are decreased, the strut mode frequency is increased, and the damping for the balance modes is reduced. For the long strut configuration, the lateral cantilever strut mode frequency is around 3.5 Hz, well above the balance mode frequencies (see Table 2). Therefore the balance mode frequencies are not lowered significantly for this configuration (note that the balance side mode frequency is expected to be about $\sqrt{2}$ times the balance longitudinal mode frequency, since there are two side force scales and one drag force scale in the balance system).

The test data show a nonlinear behavior for the damping of the balance modes. The damping for high excitation level and high response amplitude consistently was significantly lower than the damping measured at low levels (the data in Tables 1 and 2 are the values for low excitation level). Figure 12 shows the general trend, for all the configurations tested. The ratio of the balance mode damping to its value at low excitation levels correlates well with the rms value of the exciting force. The linear range extends up to 30 or 40 lb (rms), and at high excitation the damping levels off at about 40 to 50% of the low excitation value. The detailed test data are given in Appendix G. A correlation between the excitation level (broadband and discrete) and the balance drag scale motion for the longitudinal balance mode is also given in Appendix G (run 11, Table G1).

From the frequencies of the modes we may identify 1/rev and N/rev resonances for the operating range of a particular rotor, and with the data on the magnitude of the hub response assess the vibration potential of these modes. From the frequency and fixed system damping we may assess the ground resonance stability of articulated and soft-inplane hingeless rotors on this Rotor Test Apparatus. A simple ground resonance stability criterion, giving the critical rpm ranges and the lag damping required for stability, is discussed in Appendix F. More detailed calculations of the dynamic stability are recommended however.

The tables of Appendix G present in detail the shake test data for the six configurations investigated.

DISCUSSION OF ANALYSIS TECHNIQUES

Several methods were used to calculate the modal parameters from the measured transfer function. The quantities required are: the natural frequency ω_n, damping coefficient C_s, damping ratio ζ, and modal mass M (note that these parameters are related by $C_s = 2\zeta\omega_n M$).

The natural frequency was estimated using three points around the experimental peak (Appendix D). This technique gave satisfactory results.

The damping coefficient was calculated from the transfer function at a single frequency point (Appendix C), and from integrals of the transfer function through the peak (Appendix E; this method was used only for runs 17 and 18, Tables G4 and G5). Both methods worked well, and the two techniques gave comparable estimates. The experimental data (Appendix G) for the single-point calculation of C_s during discrete frequency sweeps near a resonance demonstrate that this method gives an estimate of the damping which is indeed relatively insensitive to frequency, i.e. roughly constant in the vicinity of each peak (see Appendix C). The integral method of calculating C_s is less sensitive to noise in the transfer function data, but for very close modes one must watch that the limits of integration cover only one resonant peak. With discrete or very narrow-band excitation, only the single-point estimate of C_s is applicable of course. The use of both methods is recommended to obtained the best extimate of the damping coefficient.

To calculate the damping ratio and modal mass (ζ and M), the LSE parameter identification techniques described in Appendix D were used, with four iterations after the initial estimate of the parameters, and either 5 or 10 points for the curve fit around the resonant peak. For an ideal transfer function (no noise in the data) these techniques worked well, especially the two-parameter algorithms. For real data however, i.e. an experimental transfer function measurement including noise, the methods of Appendix D were not satisfactory The one-parameter algorithm (ζ from $|H|$) did no better than the initial estimate of ζ from three points. The two-parameter algorithms (ζ and M from either $|H|$ or H) either gave little improvement over the initial estimate, or simply did not converge. The difficulty is probably due to the fact that the derivatives in the iteration formulas are singular at $\zeta = 0$. There is the possibility of better success using an algorithm to identify C_s and M from the transfer function.

The damping ratio and modal mass (ζ and M) were also calculated (for runs 17 and 18, Table G4 and G5) from integrals of the transfer function, as described in Appendix E. This technique worked well, and its continued use is recommended.

APPENDIX A

The Discrete Fourier Transform

1. References

Bendat, Julius., and Piersol, Allan G., Measurement and Analysis of Random Data, John Wiley & Sons, Inc., New York, 1966

Jenkins, Gwilym M., and Watts, Donald G., Spectral Analysis and its Applications, Holden-Day, San Francisco, 1969

2. Definition and Application

The input signal (force, f) and output signal (acceleration, a) are sampled (digitized) at rate r, until the total number of samples N is collected. The result is a discrete time series of data, at $t = n\Delta t$, $n = 0...N-1$ ($\Delta t = 1/r$, with sampling period $T = N/r$). The discrete Fourier transforms of the input and output are calculated, using Fast Fourier Transform (FFT) techniques, according to the expression:

$$X(k) = \frac{1}{N} \sum_{n=0}^{N-1} x(n) e^{-i 2\pi k n / N}$$

The result is a discrete spectrum, at the N/2 frequencies $\omega = k\Delta\omega$, $k = 0...(N/2-1)$ ($\Delta\omega = r/N = 1/T$ Hz, with a maximum frequency -- spectrum bandwidth -- of $\omega_{max} = r/2$ Hz).

The input and output transforms are multiplied then to obtain the cross-spectrum $S_{io} = \overline{F} * A$ and the input autospectrum $S_{ii} = \overline{F} * F$. The spectra S_{io} and S_{ii} are averaged over a total of K records of data. Then the system transfer function is calculated as:

$$H = a/f = \text{average } S_{io}/\text{average } S_{ii}$$

3. Relation to Continuous Fourier Transform

The Fourier transform of a continuous, non-periodic time function x(t) is defined as

$$X(\omega) = \frac{1}{2\pi} \int_{-\infty}^{\infty} x(t) e^{-i\omega t} \delta t$$

The discrete Fourier transform makes two approximations: first, a finite length record of data is transformed; and secondly, a finite number of samples are taken during the record.

With a finite length record, it is assumed that the data is periodic outside the record; hence we calculate the Fourier transform of a periodic function:

$$X_1(\omega) = \frac{1}{T} \int_0^T x(t)\, e^{-i\omega t}\, dt$$

at the discrete harmonics $\omega = 2\pi k/T$. This may be considered the Fourier transform of x(t) times the window w(t) which is open only for t = 0 to T, so

$$X_1(\omega) = \frac{1}{2\pi} \int_{-\infty}^{\infty} x(t)\, w(t)\, e^{-i\omega t}\, dt$$

$$= \int_{-\infty}^{\infty} X(\omega^*)\, W(\omega - \omega^*)\, d\omega^*$$

(using the convolution theorem). The time window is

$$w = \begin{cases} 2\pi/T & 0 < t < T \\ 0 & \text{otherwise} \end{cases}$$

so the frequency window (the Fourier transform of w) is:

$$W = \frac{\sin \omega T/2}{\omega T/2}\, e^{-i\omega T/2}$$

which has amplitude 1 and bandwidth $\Delta\omega = 2\pi/T$. Thus

$$X_1(\omega) \cong \int_{\omega - \Delta\omega/2}^{\omega + \Delta\omega/2} X(\omega^*)\, d\omega^*$$

This $\Delta\omega$ is the same as the frequency increment in the discrete spectrum. So each line in the discrete transform may be viewed as the integral of the continuous transform over the interval $\omega - \Delta\omega/2$ to $\omega + \Delta\omega/2$.

With only a finite number of samples in the record, we calculate as an approximation to X_1 the discrete transform:

$$X_2(k) = \frac{\Delta t}{T} \sum_n x(n)\, e^{-i 2\pi k n \Delta t/T}$$

(the summation being the discrete approximation of the integral). Since $\Delta t/T = 1/N$, this is identical to $X(k)$ defined in section 2 above. The finite length record means that only the discrete harmonics $\omega = k\Delta\omega$ of the transform are calculated. The finite number of samples means that the maximum frequency of the spectrum is $\omega_{max} = N/2 * \Delta\omega = r/2$ (the Nyquist frequency). It is necessary to filter the analog input and output signals with a low-pass cutoff frequency at or below ω_{max}, in order to avoid aliasing of the discrete spectrum by harmonics above the Nyquist frequency, which can not be discerned by sampling at the discrete rate r.

4. Noise

Because of process and measurement noise, we do not calculate a deterministic spectrum, but rather a statistical estimator of the spectrum. In order to reduce the noise in the estimate of the spectrum, it is necessary to average the data. Thus we take K records, and calculate the average spectrum

$$\bar{S} = \frac{1}{K} \sum S_k$$

This sample spectrum has an unbiased mean, and a variance of

$$\frac{\mathrm{Var}\,\bar{S}}{S^2} = \epsilon^2 \cong \frac{1}{K}$$

The standard deviation is thus inversely proportional to $K^{\frac{1}{2}}$ (compare with the similar result for the standard deviation of a sample mean). The total sample time is $KT = K/\Delta\omega$, so for a given time it is necessary to compromise between the accuracy of the data and the frequency increment in the spectrum. Bendat and Piersol suggest using a minimum of $K = 10$ records. The statistics of the transfer function H (the ratio of the average cross spectrum to the average input autospectrum) are more complex (the reader is directed to the references given above), but the $K^{-\frac{1}{2}}$ behavior of the spectra is sufficient for the present purposes.

5. Choice of Parameters

The parameters r, N, and K are required to define the sampling and averaging process in the analysis of the data. For a given bandwidth of the data, the sample rate r suggested is

$$r = 2.5 * \text{bandwidth data}$$

($\omega_{max} = r/2 = 1.25 *$ bandwidth). A low pass filter on the signal is also required, to avoid aliasing in the discrete transform. The number of samples N is then chosen from r and the required frequency increment in the spectrum $\Delta\omega$, as $N = r/\Delta\omega$ (FFT routines used require also that N be a power of 2). We choose $\Delta\omega$ to define the resonant peaks sufficiently, from $\Delta\omega \cong \zeta\omega_n/2$ (which gives about 5 points covering the $\frac{1}{2}$ power bandwidth of the peak; ω_n is the natural frequency and ζ the damping ratio of the mode). Finally, the number of records K is chosen for the desired accuracy (noise level) of the spectrum. At least 6 to 10 records are desired; the principle restriction of the number of records is the total sample time KN/r.

APPENDIX B

Local Maximum Discriminator

1. Problem

It is necessary to identify the resonant peaks (i.e. the natural frequencies) of the experimental transfer function. The experimental transfer function has measurement and process noise however, so it is not possible to identify the peaks by simply searching for all the local maxima of the data. An algorithm must be developed which will discriminate the true peaks from the spurious local maxima due to noise.

2. The Algorithm

We have the data for the magnitude of the transfer function, which may be written $H_e = H + h$, where H is the true value and h is random noise in the measurement. Assume h has a normal distribution with zero mean and standard deviation σ, hence probability distribution:

$$f = \frac{1}{\sigma\sqrt{2\pi}} e^{-h^2/2\sigma^2}$$

Assume $\sigma = H/K^{\frac{1}{2}}$, where K is the number of records of data in the average of the cross spectrum and input autospectrum calculated to find H (see Appendix A).

Consider then the probability of a peak at a certain frequency ω_N, i.e. the probability that $H_N - H > 0$ for all nearby frequencies. This is the probability that $h > h_N - \Delta H_e$, where $\Delta H_e = H_{e_N} - H_e$; which is:

$$P_r = \int_{-\infty}^{\infty} \int_{h_N - \Delta H_e}^{\infty} f(h) f(h_N)\, dh\, dh_N$$

$$= \frac{1}{\sigma^2 2\pi} \iint e^{-(h^2+h_N^2)/2\sigma^2}\, dh\, dh_N$$

$$= \frac{1}{\sqrt{2\pi}} \int_{\frac{\Delta H_e}{\sqrt{2}\sigma}}^{\infty} e^{-y^2/2}\, dy$$

This integral may be expressed in terms of the error function.

The product of the probability Pr evaluated at several points around ω_N is the probability that all local values of H are less than the H at ω_N. Therefore we take as a discriminator of the local maxima the parameter

$$C = \left(\prod^{m} Pr \right)^{\frac{1}{m}}$$

C is evaluated at all frequencies of the transfer function. If C is above a certain confidence level for any frequency, we consider that point a resonant peak of the transfer function.

The parameter C has the following properties. For a local maximum, $C \cong 1$, while C is near 0 for a local minimum. If $\Delta H_e = 0$ for all points (i.e. the experimental data constant), then $C = \frac{1}{2}$. Finally, with $\Delta H_e/\sigma = 1, 2,$ or 3 we obtain C = .76, .92, and .98.

3. Application

For on-line evaluation of the data (locating the resonant peaks of the transfer function and calculating the system properties there), it is better to use a rather low confidence level on the discriminator (so a few false peaks are located, which are easily discarded by the engineer), rather than to use a high confidence level which will occasionally miss a true peak because of excessive noise. It is also found that the parameter C is a more sensitive discriminator of the peaks if many points are used to evaluate C for each frequency.

For the present test, a confidence level of 65 to 70 (C above the confidence level considered an indication of a resonant peak) was satisfactory. The parameter C was calculated using 12 points ("m" in the definition of C above) around each frequency.

APPENDIX C

Fixed System Damping from Transfer Function

To evaluate the ground resonance stability of a rotor on a flexible support, it is necessary to know the damping coefficient of the modes. This may be obtained from the hub impedance by the following method. Consider the mass/spring/damper system: $M\ddot{x} + C_s\dot{x} + M\omega_n^2 x = f$. The response of the hub acceleration to the applied force is the transfer function

$$H = \frac{a}{f} = \frac{-\omega^2}{M(\omega_n^2 - \omega^2) + C_s i\omega}$$

where ω_n is the natural frequency, M the generalized mass of the mode, and C_s the damping coefficient. It follows that

$$C_s \equiv \frac{\omega \, \mathrm{Im} H}{|H|^2}$$

or

$$C_s = 195.4 \frac{\omega \, \mathrm{Im} H}{|H|^2}$$

with the dimensions $[\omega]$ = Hz, $[H]$ = g/1000 lb, $[C_s]$ = lb/fps. This is the expression used to calculate the damping of the rotor support, from the experimental measurement of the hub response.

At the resonant frequency ($\omega = \omega_n$) this result becomes $C_s = \omega/|H|$. In general the previous form is preferable however, since it holds for all ω, not just at the peak. Thus it is possible to evaluate C_s even though the calculation is not performed exactly at the peak (for multimode systems it is necessary to be at least close to the peak of course). The experimental data (Appendix G) shows that the damping calculated by this expression is quite consistent in the vicinity of the resonance of each mode.

APPENDIX D

Least Squared Error (LSE) Parameter Identification of Damping Ratio from Transfer Function

1. LSE Parameter Identification

It is desired to fit an analytic function $H(\omega, u_i)$ -- where ω is the frequency, u_i are free parameters (e.g. the damping ratio ζ), and H may be either a complex transfer function or the magnitude -- to experimental data $H_e(\omega_k)$ at the discrete frequency points ω_k. We shall find the parameters u_i to minimize the squared error

$$\epsilon = \sum_k \left| H(\omega_k) - H_e(\omega_k) \right|^2$$

For complex H, this error is the sum of the distances between H and H_e on the complex plane (Re H vs. Im H, i.e. the phase plane). The minimum ϵ is given by the solution of:

$$\frac{\partial \epsilon}{\partial u_i} = \sum_k \frac{\partial}{\partial u_i} \left| H - H_e \right|^2 = 0$$

If H is linear in the parameters, the above is a set of linear algebraic equations which may be solved directly for the parameters u_i. In the present case however, H is not a linear function of u_i, so a solution by numerical methods is necessary; we shall use Newton's method. From

$$\frac{\partial f}{\partial u_i} \cong \left.\frac{\partial f}{\partial u_i}\right|_{\vec{u}^{(n)}} + \sum_j \left(u_j^{(n+1)} - u_j^{(n)}\right) \left.\frac{\partial^2 f}{\partial u_i \partial u_j}\right|_{\vec{u}^{(n)}}$$

it follows that the iterative solution of $\partial f / \partial u_i = 0$ is

$$\vec{u}^{(n+1)} = \vec{u}^{(n)} - \left[\frac{\partial^2 f}{\partial u_i \partial u_j} \right]^{-1} \left\{ \frac{\partial f}{\partial u_i} \right\}$$

where $\vec{u}^{(n)}$ is a vector of the parameters u_i (nth iteration), and the derivatives of f are evaluated using $\vec{u}^{(n)}$.

Here $f = \sum_k |H - H_e|^2$, hence the solution of the parameter identification problem is:

$$\vec{u}^{(n+1)} = \vec{u}^{(n)} - \left[\sum_k \frac{\partial^2}{\partial u_i \partial u_j} |H - H_e|^2 \right]^{-1} \left\{ \sum_k \frac{\partial}{\partial u_i} |H - H_e|^2 \right\}$$

2. Transfer function

We shall fit the measured transfer function in the neighborhood of a resonant peak to the theoretical transfer function of a mass/spring/damper system. Considering the acceleration response to an applied force, the transfer function is

$$H = \frac{a}{f} = \frac{-\omega^2/m}{\omega_n^2 - \omega^2 + i\,2\zeta\omega\omega_n}$$

Note that in general the parameter m (mass) is a complex number, because it accounts for the influence of other modes of the system in the vicinity of any particular resonance. The magnitude of H is:

$$|H| = \frac{\omega^2/|m|}{\sqrt{(\omega^2 - \omega_n^2)^2 + (2\zeta\omega\omega_n)^2}}$$

Fitting H to the experimental data around a peak requires the identification of four parameters then: the damping ratio ζ, the natural frequency ω_n, the mass $|m|$, and the phase angle $\angle m$ (only the first three are involved in fitting the magnitude of H to the experimental data).

Because of limitation of computer core and language, we consider only the identification of one or two parameters. The following cases will be considered in detail: fitting $|H|$ to $|H_e|$ by identifying ζ; fitting $|H|$ to $|H_e|$ by identifying ζ and $|m|$; and fitting H to H_e by identifying ζ and $|m|$. An initial estimate of the parameters is required to start the iterative LSE solution. It is assumed that the initial estimate of the parameters not corrected by the LSE solution (in particular the natural frequency ω_n) is satisfactorily accurate.

3. Initial Estimate of Parameters

Assume that a resonant frequency ω_p has been found (a local maximum of $|H_e|$; see Appendix B). An initial estimate of the parameters may be obtained from the experimental data at the three points ω_p , $\omega_L = \omega_p - \Delta\omega$, and $\omega_R = \omega_p + \Delta\omega$. For small ζ and small $\omega - \omega_n$ (the usual case of interest), the transfer function is approximately

$$|H| \cong \frac{1}{2|m|\sqrt{\zeta^2 + (\frac{\omega}{\omega_n} - 1)^2}}$$

From this approximation the parameters of H may be estimated as:

$$\Delta\omega_n = \Delta\omega \frac{R_R - R_L}{2(R_R + R_L - 2R_R R_L)}$$

$$\omega_n = \omega_p + \Delta\omega_n$$

$$\zeta^2 = \frac{R_L(\Delta\omega + \Delta\omega_n)^2 - (\Delta\omega_n)^2}{(1 - R_L)\omega_n^2}$$

$$\frac{1}{m} = -H_{ep}\left(\frac{\omega_n^2}{\omega_p^2} - 1 + i\,2\zeta\frac{\omega_n}{\omega_p}\right)$$

where

$$R_L = |H_{eL}/H_{ep}|^2$$
$$R_R = |H_{eR}/H_{ep}|^2$$

4. Damping ratio from $|H|$

The LSE iterative solution is

$$\zeta_{new} = \zeta_{old} + \frac{\sum_K \frac{\partial}{\partial \zeta} (H - H_e)^2}{\sum_K -\frac{\partial^2}{\partial \zeta^2} (H - H_e)^2}$$

or

$$\zeta_{new} = \zeta_{old} / (1 - r)$$

where

$$r = \frac{\sum_K \frac{\partial}{\partial \zeta} (H - H_e)^2}{\sum_K \frac{\partial}{\partial \zeta} (H - H_e)^2 - \zeta \frac{\partial^2}{\partial \zeta^2} (H - H_e)^2}$$

$$= \frac{\sum_K \omega^4 D^{-3/2} (H_e - H)}{\sum_K \omega^6 (12 \zeta^2 \omega_n^2) D^{-5/2} (H_e - \frac{4}{3} H)}$$

$$D = (\omega^2 - \omega_n^2)^2 + (2 \zeta \omega \omega_n)^2$$

$$H = \frac{\omega^2}{m} D^{-\frac{1}{2}}$$

5. Damping ratio and Mass from $|H|$

With $\mu = 1/|m|$ and $D = (\omega^2 - \omega_n^2)^2 + (2\zeta\omega\omega_n)^2$, we have $H = \mu \omega^2 D^{-\frac{1}{2}}$. The derivatives required are:

$$A = \sum_K \frac{\partial}{\partial \zeta} (H - H_e)^2 = \sum_K (H_e - H) \mu \omega^2 D^{-3/2} \frac{\partial D}{\partial \zeta}$$

$$B = \sum_K \frac{\partial}{\partial \mu} (H_e - H)^2 = \sum_K (H_e - H) (-2\omega^2 D^{-\frac{1}{2}})$$

$$a = \sum_K \frac{\partial^2}{\partial \zeta^2}(H_e - H)^2$$
$$= \sum_K \left[(H_e - H)\mu\omega^2 \Delta^{-3/2} \frac{\partial^2 \Delta}{\partial \zeta^2} - (H_e - \tfrac{4}{3}H)\mu\omega^2 \tfrac{3}{2}\Delta^{-\frac{5}{2}} \left(\frac{\partial \Delta}{\partial \zeta}\right)^2 \right]$$

$$b = \sum_K \frac{\partial^2}{\partial \mu^2}(H_e - H)^2 = \sum_K 2\omega^4 \Delta^{-1}$$

$$c = \sum_K \frac{\partial^2}{\partial \mu \partial \zeta}(H_e - H)^2 = \sum_K (H_e - 2H)\omega^2 \Delta^{-\frac{3}{2}} \frac{\partial \Delta}{\partial \zeta}$$

and the LSE iterative solution is:

$$\begin{pmatrix} \zeta \\ \mu \end{pmatrix}_{new} = \begin{pmatrix} \zeta \\ \mu \end{pmatrix} - \begin{bmatrix} a & c \\ c & b \end{bmatrix}^{-1} \begin{pmatrix} A \\ B \end{pmatrix}$$
$$= \begin{pmatrix} \zeta \\ \mu \end{pmatrix} - \frac{1}{ab - c^2} \begin{pmatrix} Ab - Bc \\ Ba - Ac \end{pmatrix}$$

6. Damping ratio and Mass from H

Using the initial estimate of $\angle m$ and ω_n, we shall match the experimental data $H_e e^{i\angle m}$ to the complex transfer function

$$H = -\mu\omega^2 \Delta^{-1}(\omega_n^2 - \omega^2 - i\,2\zeta\omega\omega_n)$$

where $D = (\omega^2 - \omega_n^2)^2 + (2\zeta\omega\omega_n)^2$ and $\mu = 1/|m|$. Then the squared error is

$$\epsilon = \sum_K |H - H_e|^2 = \sum_K \left[\mu(\alpha + \mu\omega^4 + \beta\zeta)\Delta^{-1} + |H_e|^2\right]$$

where

$$\alpha = 2\,\mathrm{Re}H_e\,\omega^2(\omega_n^2 - \omega^2)$$
$$\beta = 2\,\mathrm{Im}H_e\,\omega^2(-2\omega\omega_n)$$

The derivatives required are:

$$A = \sum_K \frac{\partial}{\partial \zeta} |H - H_e|^2 = \sum_K \left[\mu(\alpha + \mu\omega^4 + \beta\zeta)\left(-\Delta^{-2}\frac{\partial\Delta}{\partial\zeta}\right) + \beta\mu\Delta^{-1} \right]$$

$$B = \sum_K \frac{\partial}{\partial \mu} |H - H_e|^2 = \sum_K (\alpha + 2\mu\omega^4 + \beta\zeta)\Delta^{-1}$$

$$a = \sum_K \frac{\partial^2}{\partial \zeta^2} |H - H_e|^2$$

$$= \sum_K \left[\mu(\alpha + \mu\omega^4 + \beta\zeta)\left(2\Delta^{-3}\left(\frac{\partial\Delta}{\partial\zeta}\right)^2 - \Delta^{-2}\frac{\partial^2\Delta}{\partial\zeta^2}\right) - \beta\mu 2\Delta^{-2}\frac{\partial\Delta}{\partial\zeta} \right]$$

$$b = \sum_K \frac{\partial^2}{\partial \mu^2} |H - H_e|^2 = \sum_K 2\omega^4\Delta^{-1}$$

$$c = \sum_K \frac{\partial^2}{\partial\mu\partial\zeta} |H - H_e|^2 = \sum_K \left[(\alpha + 2\mu\omega^4 + \beta\zeta)\left(-\Delta^{-2}\frac{\partial\Delta}{\partial\zeta}\right) + \beta\Delta^{-1} \right]$$

and the LSE iterative solution is:

$$\begin{pmatrix} \zeta \\ \mu \end{pmatrix}_{new} = \begin{pmatrix} \zeta \\ \mu \end{pmatrix} - \frac{1}{ab - c^2} \begin{pmatrix} Ab - Bc \\ Ba - Ac \end{pmatrix}$$

APPENDIX E

Damping Ratio from Integral of Transfer Function

The damping ratio, mass, and damping coefficient may be calculated from integrals of the system transfer function. This method is an alternative to the single point or curve fit techniques described above (Appendices C and D). Assuming a single mode transfer function:

$$H = \frac{a}{f} = \frac{-\omega^2/m}{\omega_n^2 - \omega^2 + i\,2\zeta\omega\omega_n}$$

it may be shown that the damping coefficient and mass are given by:

$$C_s = \frac{\int_0^\infty \frac{\operatorname{Im} H}{\omega}\, d\omega}{\int_0^\infty \frac{|H|^2}{\omega^2}\, d\omega}$$

$$m = \frac{\pi/2}{\int_0^\infty \frac{\operatorname{Im} H}{\omega}\, d\omega}$$

and then the damping ratio is $\zeta = C_s/2m\omega_n$.

To apply this result to experimental data, the transfer function is integrated through each mode from $0.8\omega_n$ to $1.2\omega_n$. Correcting for the finite limits, we obtain:

$$m = \frac{1510}{\int_{.8\omega_n}^{1.2\omega_n} \frac{\operatorname{Im} H}{\omega}\, d\omega}$$

$$\zeta = \frac{.33}{\omega_n} \frac{\left(\int_{.8\omega_n}^{1.2\omega_n} \frac{\operatorname{Im} H}{\omega}\, d\omega\right)^2}{\int_{.8\omega_n}^{1.2\omega_n} \frac{|H|^2}{\omega}\, d\omega}$$

$$C_s = 195.4 \; \frac{\int_{.8\omega_n}^{1.2\omega_n} \frac{\mathrm{Im}\, H}{\omega}\, d\omega}{\int_{.8\omega_n}^{1.2\omega_n} \frac{|H|^2}{\omega^2}\, d\omega}$$

with dimensions $[H]$ = g/1000 lb, $[\omega]$ = Hz, $[m]$ = lb, and $[C_s]$ = lb/fps. Note that the result for C_s is independent of the limits of integration; compare with the expression in Appendix C. For extremely close modes it may be necessary to integrate over a smaller range around ω_n; the above limits were satisfactory for the present test however. The natural frequency ω_n may be obtained from the three-point curve fit around a local maximum, as described in Appendix D, part 3.

By calculating the system parameters from integrals of the transfer function, the effect of noise in the experimental data is reduced. However, the above expressions are not unbiased estimators of ζ and C_s. With the factor $|H|^2$ in the denominator, the calculation of ζ and C_s in the presence of noise will underestimate the true values. The error in the estimate will be of the order K^{-1}, where K is the number of data records over which the spectra are averaged (see Appendix A). The estimate is conservative at least, and for the present cases the error is only 5 to 10%. If desired, the calculations of ζ and C_s may be multiplied by (K+1)/K as an approximate correction for the bias error.

APPENDIX F

Ground Resonance Stability Criterion

1. References

Coleman, Robert P., and Feingold, Arnold M., "Theory of Self-Excited Mechanical Oscillations of Helicopter Rotors with Hinged Blades," NACA Rept. 1351, 1958

Deutsch, M.L., "Ground Vibrations of Helicopters," Journal of the Aeronautical Sciences, vol. 13, no. 5, May 1946

2. Ground resonance

Ground resonance is a mechanical instability involving the coupled dynamics of the rotor lag and hub inplane motion. An instability is possible at the resonance of the low frequency lag mode (frequency $\Omega(1-\nu_\zeta)$) and a fixed system mode (frequency ω_x), if the product of the fixed system damping and the rotor blade lag damping is below a critical level dependent on the blade inertia and lag frequency.

3. Approximate stability criterion

The critical rotor speed for resonance is

$$\Omega_{crit} = \omega_x/(1-\nu_\zeta)$$

and the system damping required at resonance is

$$\left(\frac{C_x}{\omega_x^2}\right)\left(\frac{C_\zeta}{\frac{N}{4}\,S_\zeta^2\,\frac{1-\nu_\zeta}{\nu_\zeta}}\right) > 1$$

where ω_x = support natural frequency

C_x = support damping

ν_ζ = blade lag frequency (rotating)

C_ζ = lag damping

N = number of blades

S_ζ = first moment of blade mass about lag hinge (i.e. mass * radial C.G. location)

With dimensions $[\Omega]$ = rpm, $[\omega_x]$ = Hz, $[\nu_\zeta]$ = per rev, $[C_x]$ = lb/fps, $[C_\zeta]$ = ft-lb/rad/sec, and $[S_\zeta]$ = slug-ft, the stability criterion is:

$$\Omega_{crit} = \left(\frac{60}{1-\nu_\zeta}\right)\omega_x$$

$$C_\zeta > \frac{K}{C_x/\omega_x^2} \quad , \quad K = 39.4\,\frac{N}{4}\,S_\zeta^2\,\frac{1-\nu_\zeta}{\nu_\zeta}$$

Usually the required lag damping for stability (C_ζ) is increased by a margin of 30 to 50% to obtain an engineering estimate of the stability boundary.

This criterion is based on the assumption of a small ratio of blade mass to the rotor support mass, which is usually quite true. For extremely small fixed system damping this approximate criterion may not be conservative however. In general a detailed analysis of ground resonance stability is recommended.

APPENDIX G

Rotor Test Apparatus Shake Test Data

The tables of this appendix present the data for the resonant frequencies of the hub transfer functions (lateral acceleration due to lateral force, and longitudinal acceleration due to longitudinal force). The following configurations were tested:

Table G1. Short struts
Table G2. Short struts, balance locked
Table G3. Short struts, with strut dampers (8 shocks)
Table G4. Long struts
Table G5. Long struts, balance locked
Table G6. Long struts, with strut dampers (8 shocks)

The following quantities are given in the tables: the resonant frequency ω (Hz); the amplitude of the hub response H (g/1000 lb and in/1000 lb); the phase of the response $\angle H$ (degrees); the fixed system damping of the mode C_s (lb/fps); the damping ratio ζ (per-cent of critical damping); and the amplitude of the exciting force F (rms lb, with "D" indicating discrete frequency excitation). Several sweeps of discrete frequency excitation in the vicinity of resonances were made, and the data are given for the entire sweep as well as for the peak.

The hub response and damping coefficient data for the long struts, lateral shake, balance free and locked (runs 17 and 18, Tables G4 and G5) are somewhat uncertain because of a problem with the accelerometer calibration. However, the conversion factor (g/volt) used for these two runs was certainly within 25% of the correct factor. The frequency and damping ratio data are not affected by this problem.

Table G1. Short struts.

Run/ Pt	ω Hz	H g/1000 lb	H in/1000 lb	∠H deg	C_s lb/fps	ζ % critical	F rms lb D = discrete			
	longitudinal modes									
1/13	1.72	.22	.73	−107	1456	3.3	62			
2/1	1.76	.20	.69	−64	1500	1.7	68			
2	1.72	.19	.62	−97	1770	4.4	136			
3	1.75	.18	.55	−46	1430	2.7	148			
11/1	1.66	.23	.84	−113	1276	3.9	128			
10	1.61	.16	.59	−141	1262	3.8	122			
2/8	1.72	.36	1.14	−125	782		Δ 50			
9	1.72	.33	1.03	−140	676		Δ 102			
10	1.72	.39	1.23	−92	884		Δ 50			
11	1.72	.40	1.30	−101	834		Δ 58		balance drag scale	
11/3	1.70	.21		−53	1258		Δ 28		±92 lb *	
9	1.70	.38		−95	868		Δ 34		125	
4	1.70	.35		−128	742		Δ 46		140	
5	1.70	.29		−145	646		Δ 74		170	
6	1.70	.26		−151	614		Δ 106		200	
7	1.70	.26		−150	628		Δ 136		220	
								* about same amplitude motion as Run 11/Pt 1 (9 Hz bandwidth, 128 lb rms)		
1/13	3.04	.41	.44	−83	1410	1.5	62			
2/1	3.08	.44	.46	−41	884	1.0	68			
2	3.02	.37	.39	−51	1248	3.3	136			
3	3.02	.34	.38	−38	1698	2.5	149			
11/1	2.99	.34	.36	−40	1104	2.4	128			
2	3.01	.22	.24	−26	1164		266			
10	2.96	.36	.40	−49	1236	1.3	122			
2/12	3.04	.23	.25	−18	756		Δ 84			
13	3.04	.23	.25	−21	880		Δ 160			

ARC 167 ☆GPO 74 794 585/5956

Table G1. (continued)

Run/It	ω Hz	$\ddot{H}$ g/1000 lb	H in/1000 lb	$\angle$H deg	C_s lb/fps	ζ critical	F rms lb Δ = discrete
	longitudinal modes						
1/13	7.32	.16	.03	−149	4428	1.1	62
2/1	7.31	.15	.03	−145	5524	1.0	68
2	7.32	.16	.03	−139	5846	.9	136
11/1	7.28	.14	.03	−156	4128	1.8	128
2	7.34	.10	.02	−145	7702		266
10	7.32	.13	.02	−145	6200	2.0	122
2/14	7.28	.16	.03	−147	4972		Δ46
15	7.28	.15	.03	−138	6394		Δ112
	lateral modes						
3/3	2.08	.35	.79	77	1142	1.5	128
6	2.12	.36	.79	64	1028	1.7	128
7	2.08	.36	.81	15	308	.4	160
3/3	2.24	.33	.64	149	678	2.8	128
6	2.25	.36	.69	158	458	1.6	128
7	2.20	.40	.82	167	236	2.3	160

Table G1. (continued)

Run/Pt	ω Hz	H g/1000 lb	H in/1000 lb	$\angle$H deg	C_s lb/fps	ζ % critical	$\bar{F}$ rms lb D = discrete
	lateral modes						
3/2	2.20	.47	.96	156	372	1.5	74
5	2.13	.81	1.76	50	392	2.5	126
7/14	2.16	1.16	2.44	120	312	4.6	180
3/3	2.08/2.24				414 *		128
6	2.12/2.25				316 *		128
7	2.08/2.20				134 *		160
16	2.12	1.19	2.59	94	348		D 64
25	2.14	1.37	2.92	81	300		D 30
3/1	3.60	.35	.26	114	1834	1.7	64
2	3.58	.38	.29	130	1404	1.6	74
3	3.58	.36	.27	125	1618	1.9	128
5	3.54	.39	.31	123	1476	1.7	126
6	3.52	.36	.29	116	1692	2.3	128
7	3.53	.38	.31	108	1656		160
33	3.52	.32	.26	78	2066		D 76

* damping for equivalent single modes: $\frac{1}{C_{eq}} = \frac{1}{C_1} + \frac{1}{C_2}$

ARC 167

GPO 74 794 585/5956

Table G1. (continued)

Run/ Pt	ω Hz	H g/1000 lb	H in/1000 lb	$\angle$H deg	C_s lb/fps	ζ % critical	F rms lb D = discrete			
	lateral modes									
3/29	2.06	.61		27	300		Δ 38			
11	2.08	.52		29	286		Δ 24			
13	2.10	.84		44	334		Δ 36			
15	2.12	1.14		62	324		Δ 28			
25	2.14	1.37		81	300		Δ 30			
17	2.16	1.20		116	316		Δ 30			
27	2.18	1.05		135	286		Δ 34			
19	2.20	.71		153	276		Δ 30			
21	2.22	.60		157	282		Δ 38			
23	2.24	.46		163	272		Δ 34			
31	2.26	.40		165	288		Δ 46			
3/30	2.06	.59		31	348		Δ 80			
12	2.08	.70		39	366		Δ 70			
14	2.10	.93		53	352		Δ 62			
16	2.12	1.19		94	348		Δ 64			
26	2.14	1.12		115	338		Δ 70			
18	2.16	.98		126	344		Δ 68			
28	2.18	.90		136	330		Δ 62			
20	2.20	.75		145	326		Δ 72			
22	2.22	.66		152	310		Δ 76			
24	2.24	.59		158	286		Δ 74			
32	2.26	.48		163	266		Δ 74			

ARC 167

GPO 74 794 585/5956

Table G1. (concluded)

Run/ Pt	ω Hz	H g/1000 lb	H in/1000 lb	F rms lb			Run/ Pt	ω Hz	H g/1000 lb	H in/1000 lb	F rms lb
	longitudinal modes							lateral modes			
2/4	10.0	1.06	.11	86			3/8	23.0	2.93	.05	40
6		.66	.06	24			9		2.95	.05	60
7		.92	.10	62			10		2.94	.05	78
2/4	14.1	.69	.04	86			3/8	27.3	2.49	.03	40
6		.71	.04	24			9		2.31	.03	60
7		.75	.04	62			10		2.19	.03	78
2/4	25.2	3.28	.05	86							
6		2.97	.04	24							
7		3.05	.05	62							
2/4	28.5	1.54	.02	86							
6		1.50	.02	24							
7		1.40	.02	62							
2/4	31.0	1.69	.02	86							
6		1.91	.02	24							
7		1.45	.02	62							
2/4	35.0	2.10	.02	86							
6		2.22	.02	24							
7		1.52	.02	62							

☆GPO 74 794 585/5956

Table G2. Short struts, balance locked.

Run/ Pt	ω Hz	H g/1000 lb	H in/1000 lb	$\angle$H deg	C_s lb/fps	ζ % critical	F rms lb D = discrete			
	longitudinal modes									
10/8	2.32	.33	.60	-23	540	1.9	156			
9	2.27	.79	1.50	-52	444	2.1	150			
13	2.26	.76	1.44	-46	418	2.3	130			
10/8	7.92	.19	.03	-154	3404	1.2	156			
9	7.97	.21	.03	-145	4158	1.5	150			
13	7.97	.20	.03	-141	4832	1.7	130			
	lateral modes									
9/1	2.45	1.25	2.03		384		68			
2	2.45	1.63	2.63	76	282	1.6	146			
3	2.46	1.26	2.01	153	176	1.9	142			
6	2.45	.79	1.31	151	290		D 72			

ORIGINAL PAGE IS OF POOR QUALITY

ARC 167

GPO 74 794 585/5956

Table G2. (concluded)

Run/Pt	ω Hz	H g/1000 lb	H in/1000 lb	F rms lb			Run/Pt	ω Hz	H g/1000 lb	H in/1000 lb	F rms lb
	longitudinal modes							lateral modes			
10/6	10.1	.90	.08	28			9/4	23.4	1.78	.03	36
7	10.0	.74	.07	80			5	23.0	2.22	.04	76
10/6	15.4	.52	.02	28			9/4	28.5	1.92	.02	36
7	15.3	.48	.02	80			5	26.9	1.85	.02	76
10/6	26.2	2.42	.04	28							
7	25.3	2.48	.04	80							
10/6	31.5	1.30	.02	28							
[illegible]	31.2	1.29	.02	80							
10/6	35.0	1.47	.01	28							
7	35.2	1.50	.01	80							

Table G3. Short struts, with strut dampers (8 shocks).

Run/Pt	ω Hz	H g/1000 lb	H in/1000 lb	$\angle$H deg	C_s lb/fps	ζ % critical	F rms lb D = discrete			
	longitudinal modes									
12/1	1.65	.09	.32	−105	3442	4.4	64			
2	1.68	.09	.30	−102	3652	4.0	132			
3	1.70	.09	.30	−92	3702	5.4	104			
9	1.70	.10	.35	−135	2298		Δ 38			
10	1.70	.07	.24	−135	3308		Δ98			
11	1.70	.08	.26	−132	3192		Δ160			
12/1	4.96	.25	.10	−117	3476	1.2	64			
2	4.81	.15	.06	−96	6398	1.1	132			
3	5.0	.16	.06		6100		104			
12	5.00	.29	.12	−110	3138		Δ 38			
13	5.00	.12	.04	−91	8634		Δ100			
14	5.00	.09	.03	−89	10900		Δ134			
12/1	5.96	.23	.07	−103	4790	.9	64			
2	5.70	.13	.04	−109	8486	.7	132			
3	5.70	.13	.04	−115	7948	.9	104			
15	5.80	.27	.08	−111	3906		Δ42			
16	5.80	.12	.04	−91	9466		Δ100			
12/1	7.56	.08	.02	−112	16556		64			
2	7.64	.10	.02	−146	8632		132			

ARC 167

☆GPO 74 794 585/5956

Table G3. (continued)

Run/ Pt	ω Hz	H g/1000 lb	H in/1000 lb	$\angle$H deg	C_s lb/fps	ζ % critical	F rms lb D = discrete			
	longitudinal modes									
12/19	5.08	.12		−80	8390		D 102			
18	5.04	.12		−86	8344		D 102			
13	5.00	.12		−91	8634		D 100			
17	4.96	.12		−94	8130		D 100			
20	4.92	.13		−94	7436		D 94			
21	4.88	.13		−93	7192		D 96			
22	4.84	.13		−98	6850		D 92			
23	4.80	.14		−97	6662		D 94			
24	4.76	.14		−105	6364		D 92			
25	4.72	.14		−108	6244		D 94			
26	4.68	.14		−113	5766		D 90			
12/12	5.00	.29		−110	3138		D 18			
27	4.76	.19		−164			D 27			
12/14	5.00	.09		−88	10910		D 67			
12/28	4.76	.09		−88	10466		D 77			

ARC 167

GPO 4 794 585/5956

Table G3. (continued)

Run/ Pt	ω Hz	H g/1000 in	H in/1000 lb	$\angle$H deg	c_s lb/fps	ζ % critical	F rms lb D = discrete
	lateral modes						
8/1	1.95	.20	.50		1952		64
2	1.95	.18	.46		2120		156
3	1.90	.20	.54		1856		134
10	1.95	.21	.53		1818		166
11	1.88	.25	.70	72	1380	3.9	122
13	1.88	.42	1.17	60	752		D 30
8/1	2.15	.16	.32		2720		64
2	2.2	.21	.42		2040		156
3	2.20	.20	.41		2100		134
10	2.15	.21	.46		1954		166
11	2.20	.19	.39		2240		122
24	2.32	.14	.25	146	1860		D 50
8/2	3.54	.22	.18	108	2898	1.8	156
3	3.53	.23	.18	101	2956	2.4	134
10	3.6	.21	.16		3258		166
11	3.52	.18	.14	123	3208	2.3	122
28	3.58	.13	.10	135	3654		D54

Table G3. (continued)

Run/ Pt	ω Hz	H g/1000 lb	H in/1000 lb	$\angle$H deg	C_s lb/fps	ζ % critical	F rms lb D = discrete		
	lateral modes								
8/12	1.84	.31		41	758		D 26		
13	1.88	.42		60	752		D 30		
14	1.92	.31		89	1202		D 42		
15	1.96	.26		109	1380		D 44		
16	2.00	.22		119	1586		D 50		
17	2.04	.17		126	1836		D 54		
18	2.08	.14		141	1862		D 54		
19	2.12	.12		139	2244		D 58		
20	2.16	.10		150	2212		D 54		
21	2.20	.09		141	2938		D 52		
22	2.24	.10		134	2974		D 60		
23	2.28	.11		138	2772		D 52		
24	2.32	.13		146	1860		D 50		
25	2.36	.12		185			D 58		
8/27	3.50	.11		119	5514		D 50		
26	3.54	.12		130	4206		D 50		
28	3.58	.13		135	3654		D 54		
29	3.62	.12		131	4444		D 50		

ARC 167

GPO 74 794 585/5956

Table G3. (concluded)

Run/ Pt	ω Hz	H g/1000 lb	H in/1000 lb	F rms lb			Run/ Pt	ω Hz	H g/1000 lb	H in/1000 lb	F rms lb
	longitudinal modes							lateral modes			
12/7	10.6	.77	.07	30			8/8	23.4	3.48	.07	34
8	10.9	.82	.07	74							
12/7	15.7	.57	.03	30			8/8	28.2	3.35	.04	34
8	15.4	.50	.02	74							
12/7	26.2	3.09	.05	30							
8	25.6	3.34	.05	74							
12/7	29.0	1.55	.02	30							
8	28.5	1.60	.02	74							
12/7	31.4	1.69	.02	30							
8	31.0	1.74	.02	74							
12/7	35.0	1.90	.01	30							
8	35.2	2.07	.01	74							

ARC 167

GPO 74 794 585/5956

Table G4. Long struts.

Run/Pt	ω Hz	H g/1000 lb	H in/1000 lb	∠H deg	C_s lb/fps	ζ % critical	F rms lb D = discrete
	longitudinal modes						
13/6	1.56	.08	.33	77	3544	3.2	44
7	1.67	.08	.28	91	3966	2.3	120
8	1.63	.09	.35		3344		118
26	1.84	.20	.57	48	1346		Δ 100
45	1.98	.32	.78	95	1220		Δ 188
13/6	4.04	.75	.45	142	648	1.3	44
7	4.02	.78	.47	126	802	2.5	120
8	4.01	1.07	.65	69	678	1.3	118
54	4.03	1.46	.87	100	532		Δ 64
13/6	7.20	.09	.01	25	6530	1.3	44
13/47	3.84	.38	.25	20	686		Δ 102
48	3.92	.51	.38	29	622		Δ 100
49	3.96	.76	.47	40	686		Δ 108
50	4.00	1.36	.83	70	538		Δ 60
53	4.01	1.44	.88	76	526		Δ 58
54	4.03	1.46	.98	100	532		Δ 64
51	4.04	1.32	.79	132	446		Δ 56
52	4.08	.54	.32	169			Δ 58

ARC 167

GPC 74 794 585/5956

Table G4. (continued)

Run/Ft	ω Hz	H g/1000 lb	H in/1000 lb	$\angle$H deg	C_s lb/fps	ζ % critical	F rms lb D = discrete			
	longitudinal modes									
13/18	1.52	.05	.22	17	1690		D 98			
19	1.56	.05	.22	17	1594		D 114			
20	1.60	.06	.26	19	1528		D 106			
21	1.64	.08	.31	25	1568		D 88			
22	1.68	.10	.34	29	1592		D 92			
23	1.72	.11	.36	30	1562		D 112			
24	1.76	.13	.42	36	1502		D 102			
25	1.80	.16	.48	40	1404		D 104			
26	1.84	.19	.57	48	1346		D 100			
34	1.85	.08	.23	148	2352		D 82			
27	1.88	.06	.18	154	2442		D 100			
30	1.88	.05	.14	156	2950		D 98			
35	1.91	.02					D 100			
31	1.92	.03	.10	159	3608		D 118			
36	1.93	.02								
29	1.96	.02	.05	158	7220		D 124			
32	2.00	.01					D 108			
33	2.04	.01					D 96			
13/39	1.80	.12	.36	26	1318		D 190			
37	1.84	.15	.43	31	1240		D 184			
41	1.88	.18	.52	38	1204		D 170			
42	1.92	.25	.67	53	1186		D 188			
43	1.96	.31	.80	77	1180		D 182			
44	2.00	.19	.46	139	1348		D 168			
45	2.00	.32	.78	95	1224		D 188			
46	2.04	.05	.11	160	2840		D 236			

Table G4. (continued)

Run/ Pt	ω Hz	H g/1000 lb	H in/1000 lb	∠H deg	C_s lb/fps	ζ % critical	F rms lb Δ = discrete		Modal Mass M lb	
	lateral modes									
17/1	2.31	.22	.40	−126.5	1658	5.5	62		74500	
2	2.32	.20	.38	−107	2082	5.8	116		74800	
14	2.52	.41	.64	−122	1010		Δ 86			
25	2.38	.26	.45	−112	1640		Δ 44			
17/1	2.68	.20	.28	−70	2378	4.6	62		52800	
2	2.66	.16	.22	−96	3358	4.6	116		58600	
17/1	4.51	1.29	.62	−89	534	.8	62		37600	
2	4.49	1.18	.58	−109	616	.9	116		40000	
32	4.50	1.30	.62	−81	672	1.0	Δ 38		37900	
26	4.48	.92	.45	−85	936		Δ 64			
17/33	4.44	.86	.47	−137	616		Δ 44			
28	4.48	1.27	.62	−100	682		Δ 40			
32	4.50	1.30	.62	−81	672		Δ 38			
29	4.52	1.19	.57	−55	606		Δ 44			
26	4.48	.93	.45	−85	936		Δ 64			

ARC 167

☆GPO 74 794 ·85/5956

Table G4. (continued)

Run/ Pt	ω Hz	H g/1000 lb	H in/1000 lb	$\angle H$ deg	C_s lb/fps	ζ % critical	F rms lb D = discrete			
	lateral modes									
17/6	2.12	.08	.18	−166	1246		D 100			
7	2.20	.11	.22	−163	1186		D 98			
8	2.24	.12	.25	−160	1168		D 94			
9	2.28	.15	.28	−157	1192		D 94			
10	2.32	.17	.30	−155	1132		D 100			
11	2.36	.20	.35	−149	1198		D 94			
12	2.40	.22	.36	−146	1234		D 98			
13	2.44	.25	.41	−144	1108		D 106			
21	2.48	.30	.47	−135	1144		D 104			
14	2.52	.42	.64	−122	1010		D 86			
17	2.53	.09	.15	−45	3630		D 88			
16	2.56	.06	.12	−59			D 94			
17/23	2.32	.20	.38	−139	1464		D 50			
22	2.36	.23	.42	−119	1706		D 48			
25	2.38	.26	.45	−112	1640		D 44			
18	2.40	.25	.43	−96	1826		D 46			
24	2.42	.19	.30	−59	2222		D 44			
19	2.44	.12	.20	−52	3092		D 48			

ARC 167

GPO 74 794 58/595

Table G4. (concluded)

Run/Pt	ω Hz	H g/1000 lb	[illegible] in/1000 lb	[illegible] rms lb			Run/Pt	ω Hz	H g/1000 lb	H in/1000 lb	F rms lb
	longitudinal modes							lateral modes			
13/9	10.6	.62	.05	42			17/3	22.7	1.01	.02	30
10		.75	.06	52							
13/9	14.1	.65	.03	42			17/3	28.8	2.51	.03	30
10		.61	.03	52							
13/9	25.9	2.37	.04	42							
13/10		2.50	.04	52							
13/9	28.0	1.6	.02	42							
10		1.6	.02	52							
13/9	31.4	1.38	.02	42							
10	31.0	1.47	.02	52							
13/9	35.2	1.58	.01	42							
10		1.50	.01	52							

Table G5. Long struts, balance locked.

Run/ Pt	ω Hz	H g/1000 lb	H in/1000 lb	∠H deg	c_s lb/fps	ζ % critical	F rms lb D = discrete		Modal Mass M lb	
	longitudinal modes									
14/1	3.09	.58	.60	118	912	1.6	106			
3	3.07	1.04	1.07	135	408	1.0	154			
9	3.00	1.28	1.39	83	454		Δ 70			
14/1	7.8	.15	.02		10160		106			
3	7.73	.16	.02	49	6760		154			
14/11	2.96	.74	.82	33	422		Δ 86			
13	2.99	1.19	1.30	64	442		Δ 68			
9	3.00	1.28	1.39	83	454		Δ 70			
12	3.01	1.20	1.30	102	480		Δ 78			
10	3.04	1.05	1.11	130	432		Δ 82			
	lateral modes									
18/1	3.48	1.44	1.16	−24	272	.6	64		32000	
2	3.44	1.63	1.35	−46	286	.8	118		27400	
7	3.40	1.90	1.60	−56	292	1.0	Δ 22		26300	
18/8	3.30	.07	.60	−161	298		Δ 32			
9	3.36	1.62	1.40	−135	286		Δ 22			
7	3.40	1.90	1.60	−56	292		Δ 22			
11	3.42	1.47	1.22	−39	290		Δ 28			
10	3.44	1.26	1.04	−30	262		Δ 30			

ORIGINAL PAGE IS OF POOR QUALITY

GPO 74 794 585/5956

Table G5. (concluded)

Run/ Pt	ω Hz	H g/1000 lb	H in/1000 lb	F rms lb			Run/ Pt	ω Hz	H g/1000 lb	H in/1000 lb	F rms lb
	longitudinal mode							lateral modes			
14/4	10.2	.82	.08	44			18/3	24.6	1.80	.03	28
5		.86	.08	96			4	22.1	1.35	.02	52
14/4	15.0	.61	.02	44			18/3	28.2	2.65	.03	28
5	15.4	.56	.02	96			4	28	1.75	.02	52
14/4	24.0	2.25	.04	44							
5	24.5	2.10	.04	96							
14/4	31.4	1.28	.02	44							
5	31.0	1.22	.02	96							
14/4	35	1.30	.01	44							
5	35	1.40	.01	96							

Table G6. Long struts, with strut dampers (8 shocks)

Run/ Pt	ω Hz	H g/1000 lb	H in/1000 lb	$\angle$ H deg	C_s lb/fps	ζ % critical	F rms lb D = discrete			
	longitudinal modes									
15/1	1.57	.07	.28	49	3384		88			
2	1.6	.08	.30		3908		120			
3	1.65	.07	.24		4780		150			
14	1.92	.17	.47	77	2064		D 78			
22	1.99	.22	.54	88	1774		D 216			
30	1.78	.13	.40	109	2464		D 38			
15/1	3.62	.10	.07	35	4364	2.0	88			
2	3.6	.10	.07		7040		120			
3	3.6	.11	.08		6400		150			
33	3.61	.07	.05	61	8830		D 230			
35	3.48	.08	.06	37	2510		D 256			
15/1	5.49	.33	.10	74	3158		88			
2	5.49	.31	.10	95	3462		120			
3	5.48	.22	.07	102	4714		150			
43	4.40	.18	.10	91	4704		D 210			
15/1	7.36	.08	.02	68	17182		88			
2	7.4	.08	.02		19200		120			

ORIGINAL PAGE IS OF POOR QUALITY

ARC 167

GPO 74 794 585/5956

Table G6. (continued)

Run/ Pt	ω Hz	H g/1000 lb	H in/1000 lb	$\angle H$ deg	C_s lb/fps	ζ critical	F rms lb D = discrete			
	longitudinal modes									
15/9	1.60	.05		24	2810		D 204			
10	1.72	.07		35	2700		D 174			
11	1.80	.11		47	2456		D 142			
12	1.84	.13		56	2314		D 134			
13	1.88	.16		63	2142		D 160			
17	1.91	.17		74	2120		D 154			
14	1.92	.18		77	2064		D 156			
18	1.93	.05					D 124			
16	1.96	.07		142	3546		D 154			
15	2.00	.01					D 138			
15/19	1.92	.17		64	1974		D 212			
20	1.96	.20		70	1808		D 222			
22	1.99	.22		88	1774		D 216			
21	2.00	.21		102	1816		D 210			
15/26	1.68	.10		44	2330		D 50			
27	1.72	.10		45	2326		D 58			
28	1.76	.15		72	2278		D 40			
29	1.77	.13		61	2282		D 50			
30	1.79	.13		109	2464		D 38			
25	1.80	.05		153	3356		D 58			
24	1.92	.01					D 72			
23	1.99	.01					D 102			

Table G6. (continued)

Run/ Pt	ω Hz	H g/1000 lb	H in/1000 lb	∠H deg	C_s lb/fps	ζ %critical	F rms lb D = discrete			
	longitudinal modes									
15/31	3.60	.07		68	9658		D 194			
33	3.61	.07		61	8830		D 230			
32	3.64	.06		60	9636		D 222			
15/36	3.60	.08		28	4034		D 256			
35	3.48	.08		37	5020		D 256			
34	3.61	.08		56	7968		D 264			
15/44	4.20	.15		60	4946		D 202			
43	4.40	.19		91	4704		D 210			
42	4.72	.15		107	6138		D 196			
41	5.00	.11		110	7928		D 204			
40	5.20	.10		114	9108		D 218			
39	5.40	.09		114	10760		D 224			
38	5.44	.09		114	11240		D 276			
37	5.48	.09		113	11114		D 212			

ORIGINAL PAGE IS OF POOR QUALITY

ARC 167

☆G P O 74 794 585/4956

Table G6. (continued)

Run/ Pt	ω Hz	H g/1000 lb	H in/1000 lb	∠H deg	C_s lb/fps	ζ % critical	F rms lb D = discrete			
	lateral modes									
16/1	2.3	.25	.46		1796		116			
2	2.32	.23	.42	-77	1884	2.8	136			
3	2.34	.13	.23	-80	3484	3.1	316			
10	2.49	.25	.38	-104	1932		Δ 104			
13	2.56	.35	.51	-99	1430		Δ 156			
17	2.40	.32	.56	-74	1416		Δ 44			
16/1	4.7	.30	.13		3060		116			
2	4.7	.35	.16		2672		136			
3	4.64	.31	.15	-76	2806	1.5	316			
25	4.49	.62	.30	-85	1392		Δ 54			
29	4.55	.83	.39	-105	1034		Δ 92			
16/6	2.32	.12		-113	3360		Δ 98			
7	2.40	.16		-111	2610		Δ 98			
8	2.48	.23		-105	2030		Δ 100			
10	2.49	.25		-104	1932		Δ 104			
9	2.52	.10		-10			Δ 96			
16/11	2.49	.25		-122	1676		Δ 154			
12	2.52	.29		-115	1546		Δ 156			
13	2.56	.35		-99	1430		Δ 156			
14	2.60	.07		-22	2480		Δ 166			

Table G6. (continued)

Run/Pt	ω Hz	q g/1000 lb	H in/1000 lb	$\angle$H deg	c_s lb/fps	ζ critical	F rms lb D = discrete			
	lateral modes									
16/15	2.32	.20		-110	2146		D 48			
16	2.36	.18		-102	2426		D 56			
18	2.39	.31		-77	1476		D 42			
17	2.40	.32		-74	1416		D 44			
16/26	4.44	.53		-107	1556		D 56			
23	4.48	.46		-100	1874		D 46			
25	4.49	.62		-85	1392		D 54			
24	4.51	.60		-77	1418		D 54			
22	4.52	.54		-80	1592		D 46			
21	4.60	.46		-53	1566		D 52			
20	4.68	.35		-49	1954		D 48			
19	4.80	.28		-38	2108		D 54			
16/27	4.49	.70		-99	1236		D 76			
29	4.54	.83		-105	1034		D 92			
30	4.56	.80		-116	998		D 86			
31	4.60	.69		-133	958		D 84			
16/1	3.2	.03	.03		31000		116			
2	3.2	.02	.02		21000		136			

Table G6. (concluded)

Run/ Pt	ω Hz	H g/100 lb	H in/1000 lb	F rms lb			Run/ Pt	ω Hz	H g/1000 lb	H in/1000 lb	F rms lb
	longitudinal modes							lateral modes			
15/4	10.9	.68	.05	40			16/34	23.7	1.90	.04	28
5	10.6	.97	.08	80			35	23.4	2.10	.04	86
15/4	15.7	.67	.02	40			16/34	27.8	2.75	.03	28
5	15.4	.61	.02	30			35	27.5	7.62	.03	86
15/4	24.5	2.4	.04	40							
5	25	2.55	.04	80							
15/4	28.5	1.4	.02	40							
5		1.4	.02	80							
15/4	31.4	1.42	.02	40							
5	31.0	1.38	.02	80							
15/4	35	1.3	.01	40							
5		1.35	.01	80							

ARC 167

☆GPO 74 794 585/5956

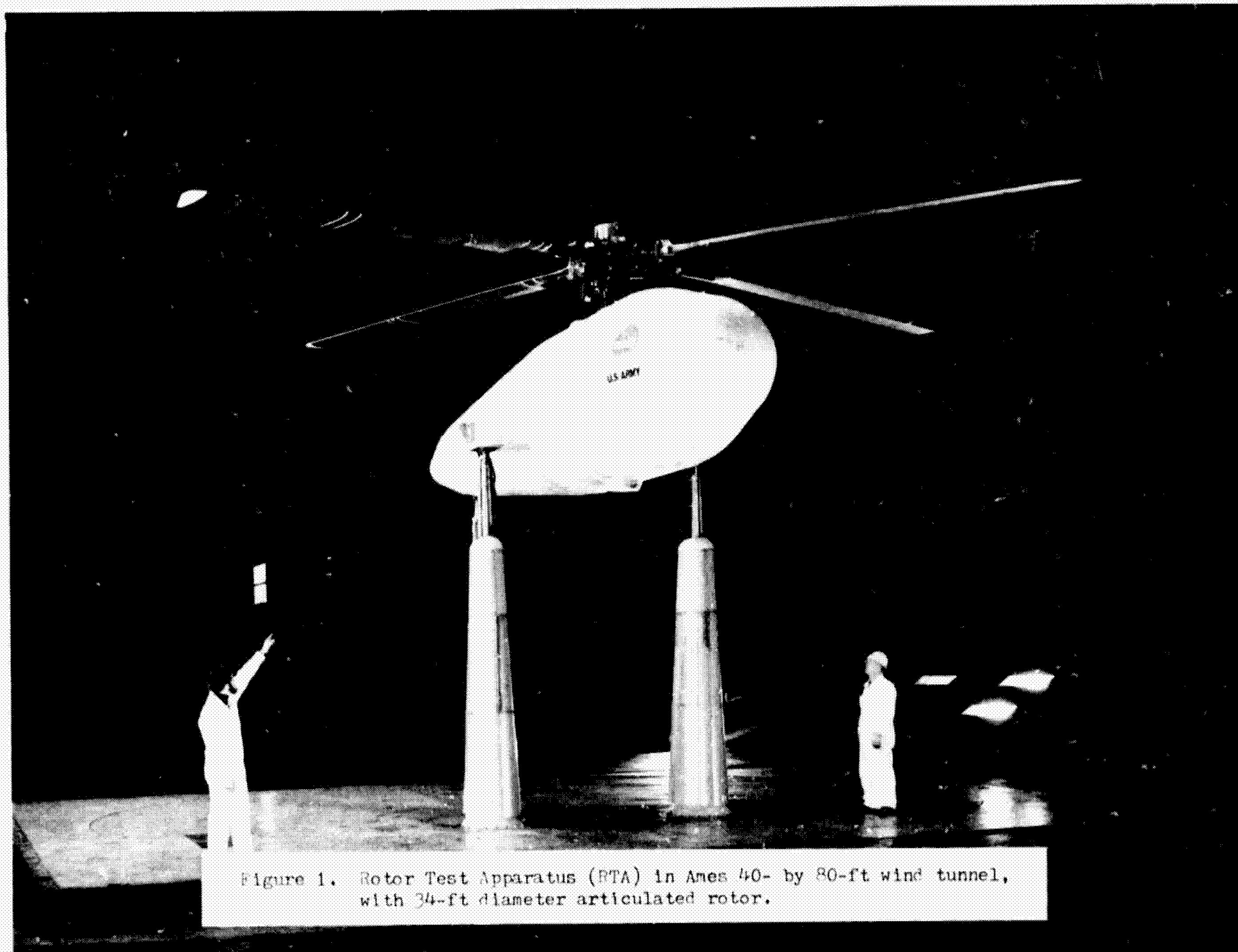

Figure 1. Rotor Test Apparatus (RTA) in Ames 40- by 80-ft wind tunnel, with 34-ft diameter articulated rotor.

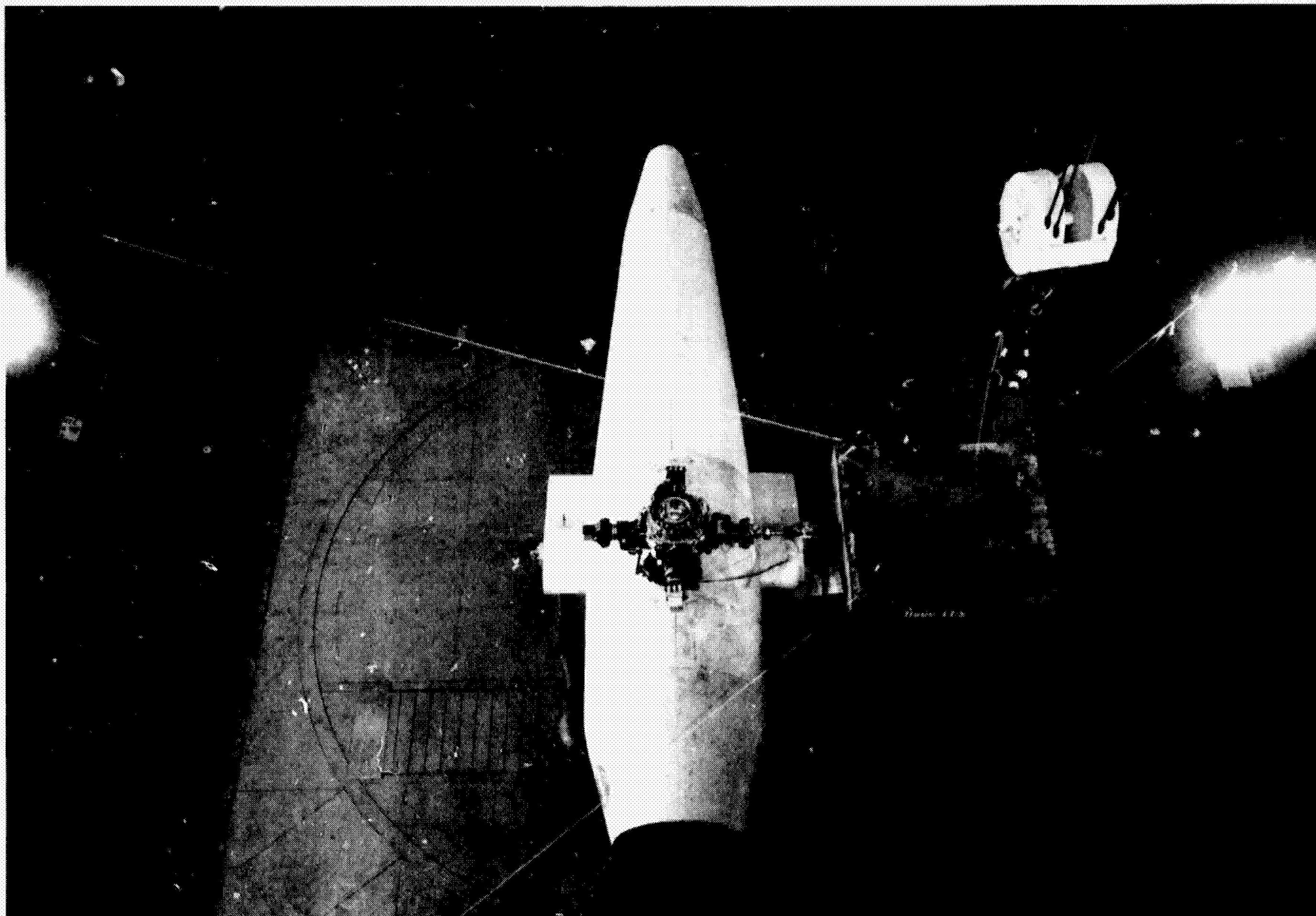

Figure 2. Shake test configuration for obtaining transfer function of rotor hub (lateral excitation), showing reaction mass and shaker.

Figure 3. Dynamic Analysis System (DAS), which was utilized in on-line analysis of the shake test data.

.5

H
g/1000 lb

0

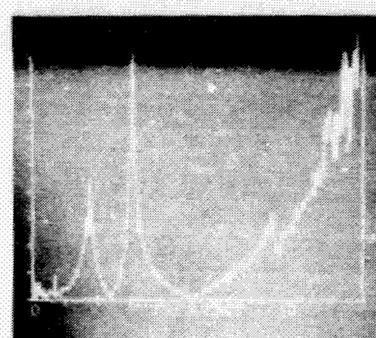

hub force
34 lb (rms)
(run 2, point 1)

.5

H
g/1000 lb

0

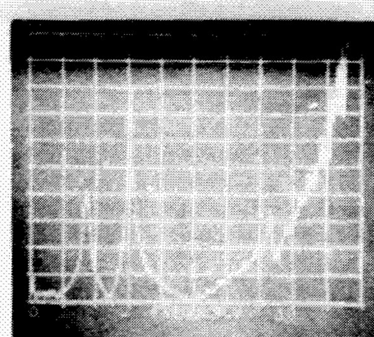

hub force
68 lb (rms)
(run 2, point 2)

.5

H
g/1000 lb

0

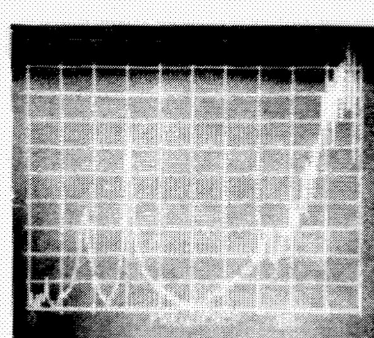

hub force
74 lb (rms)
(run 2, point 3)

Figure 4. Repeatibility of transfer function measurement. Short struts, .5-9 Hz broadband excitation, longitudinal hub response.

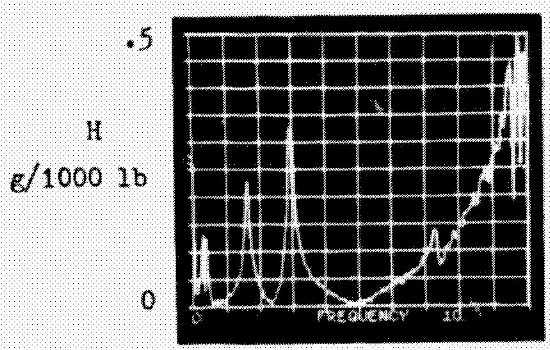

.5-9 Hz broadband excitation, longitudinal hub response

(run 11, point 1)

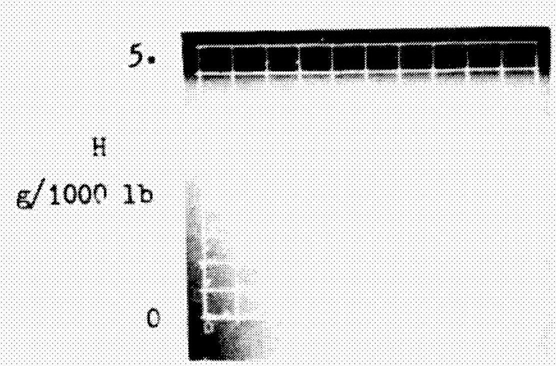

.5-35 Hz broadband excitation, longitudinal hub response

(run 2, point 7)

Figure 5. Short struts.

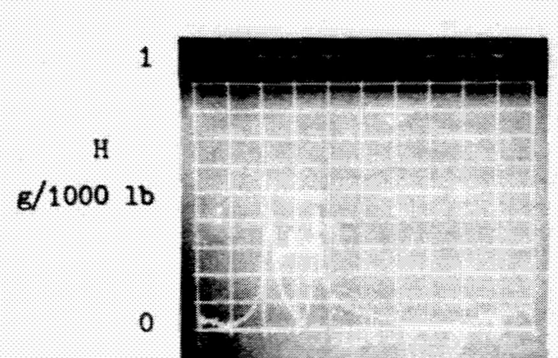

.5-9 Hz broadband excitation, lateral hub response

(run 3, point 2)

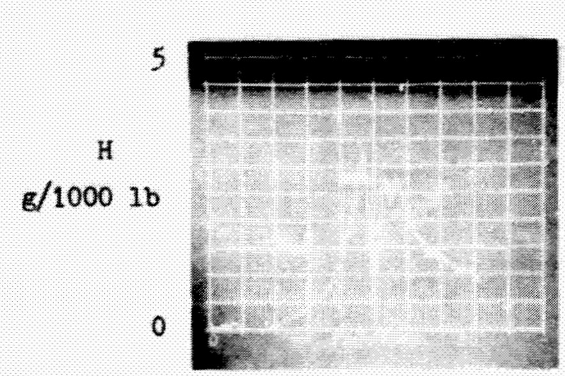

.5-35 Hz broadband excitation, lateral hub response

(run 3, point 9)

Figure 5. (concluded)

1

H

g/1000 lb

0

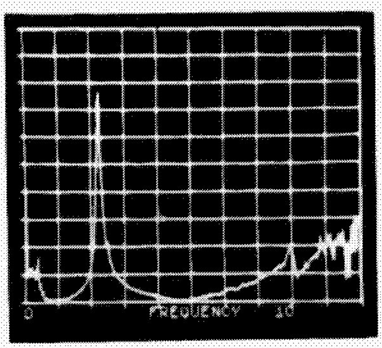

.5-9 Hz broadband excitation, longitudinal hub response

(run 10, point 13)

2.5

H

g/1000 lb

0

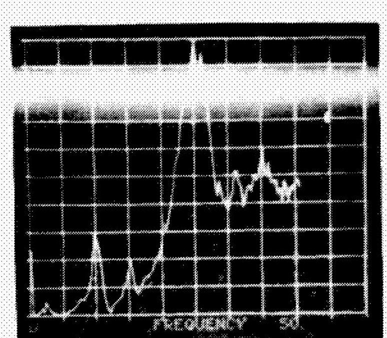

.5-35 Hz broadband excitation, longitudinal hub response

(run 10, point 7)

Figure 6. Short struts, balance locked.

2.5

H

g/1000 lb

0

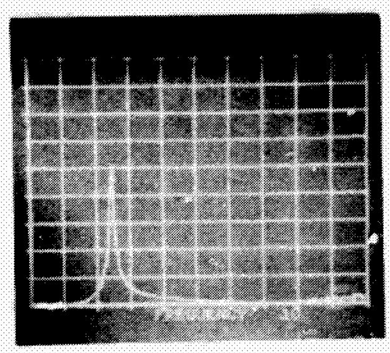

.5-9 Hz broadband excitation, lateral hub response
(run 9, point 3)

2.5

H

g/1000 lb

0

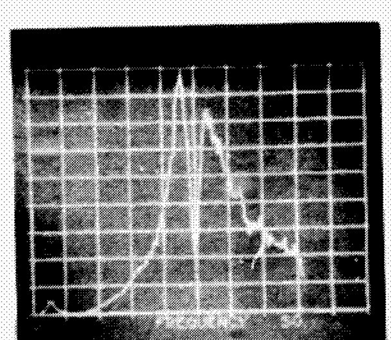

.5-35 Hz broadband excitation, lateral hub response
(run 9, point 5)

Figure 6. (concluded).

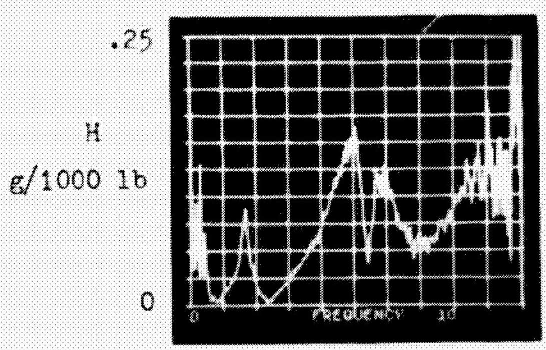

.5-9 Hz broadband excitation, longitudinal hub response
(run 12, point 3)

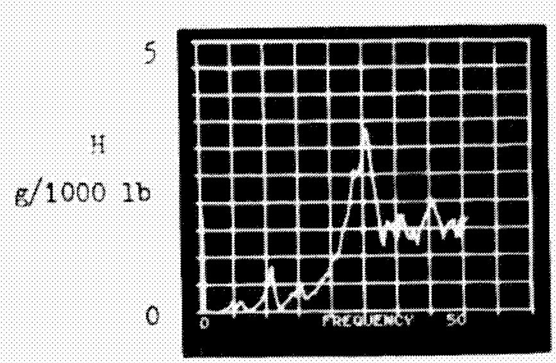

.5-35 Hz broadband excitation, longitudinal hub response
(run 12, point 8)

Figure 7. Short struts, with strut dampers (8 shocks).

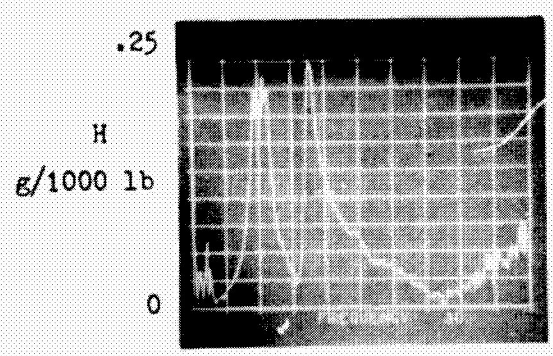

.5-9 Hz broadband excitation, lateral hub response
(run 8, point 3)

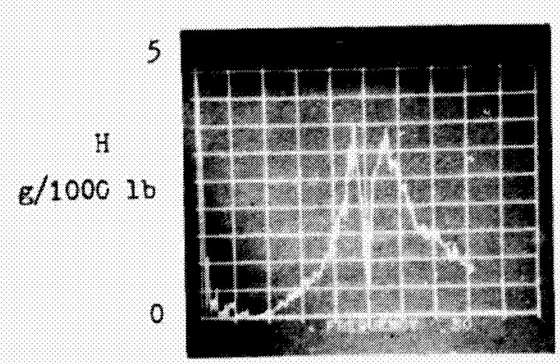

.5-35 Hz broadband excitation, lateral hub response
(run 8, point 8)

Figure 7. (concluded)

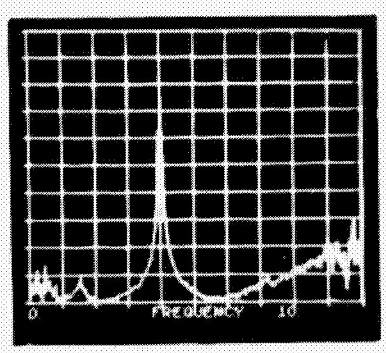

.5-9 Hz broadband excitation, longitudinal hub response
(run 13, point 6)

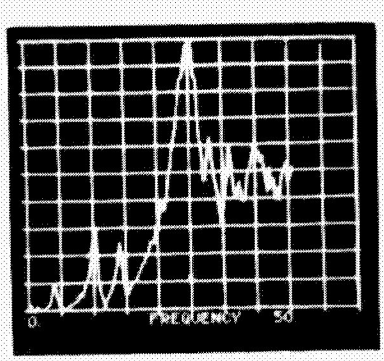

.5-35 Hz broadband excitation, longitudinal hub response
(run 13, point 10)

Figure 8. Long struts.

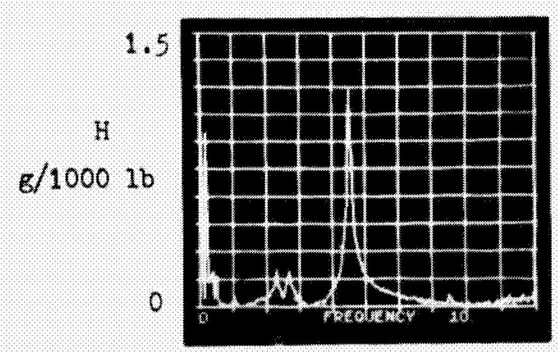

.5-9 Hz broadband excitation, lateral hub response

(run 17, point 1)

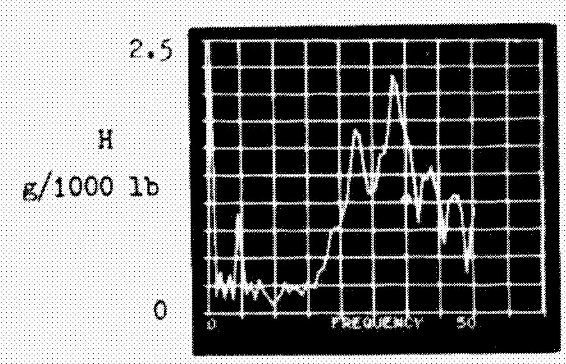

.5-35 Hz broadband excitation, lateral hub response

(run 17, point 4)

Figure 8. (concluded)

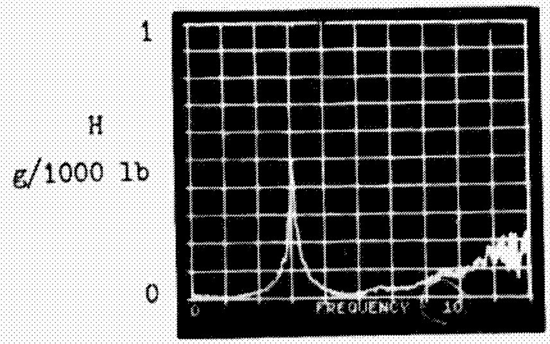

.5-9 Hz broadband excitation, longitudinal hub response

(run 14, point 2)

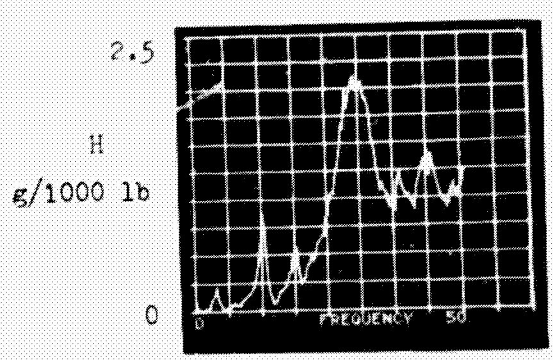

.5-35 Hz broadband excitation, longitudinal hub response

(run 14, point 5)

Figure 9. Long struts, balance locked.

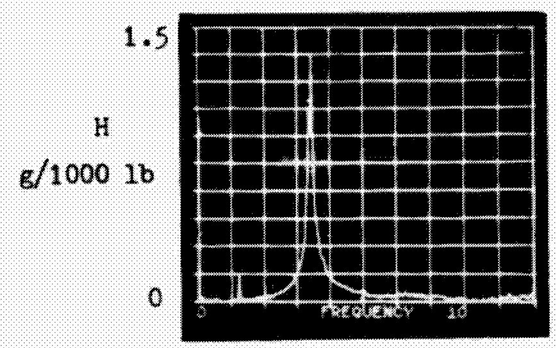

.5-9 Hz broadband excitation, lateral hub response
(run 18, point 2)

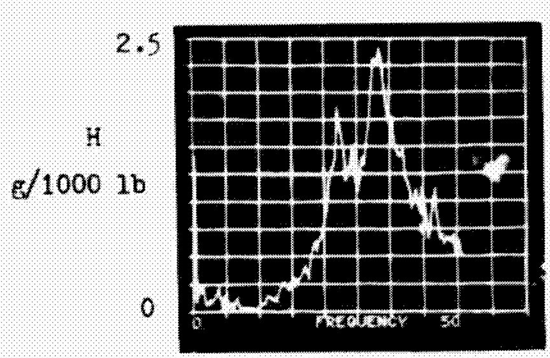

.5-35 Hz broadband excitation, lateral hub response
(run 18, point 4)

Figure 9. (concluded)

.5

H
g/1000 lb

0

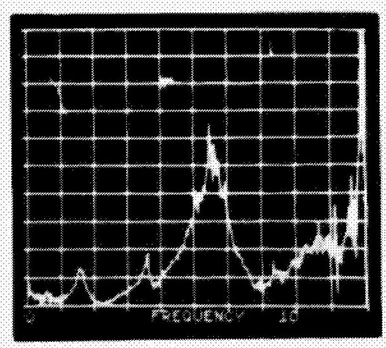

.5-9 Hz broadband excitation, longitudinal hub response
(run 15, point 1)

2.5

H
g/1000 lb

0

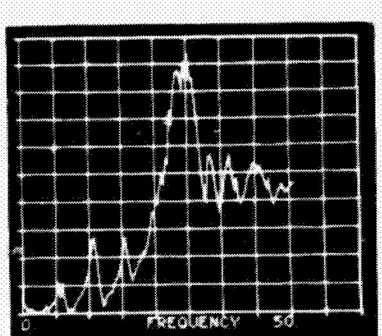

.5-35 Hz broadband excitation, longitudinal hub response
(run 15, point 4)

Figure 10. Long struts, with strut dampers (8 shocks).

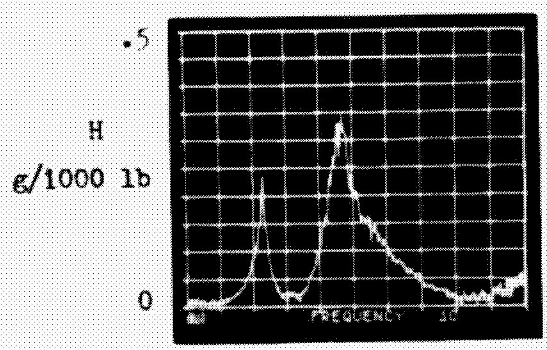

.5-9 Hz broadband excitation, lateral hub response
(run 16, point 2)

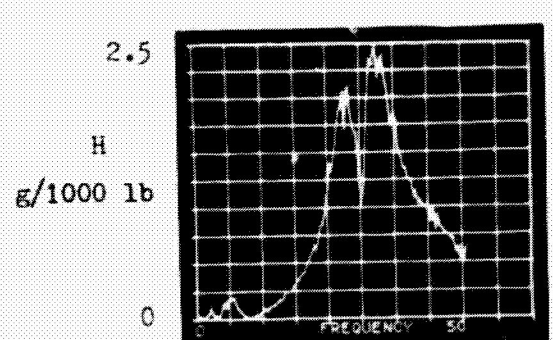

.5-35 Hz broadband excitation, lateral hub response
(run 16, point 35)

Figure 10. (concluded)

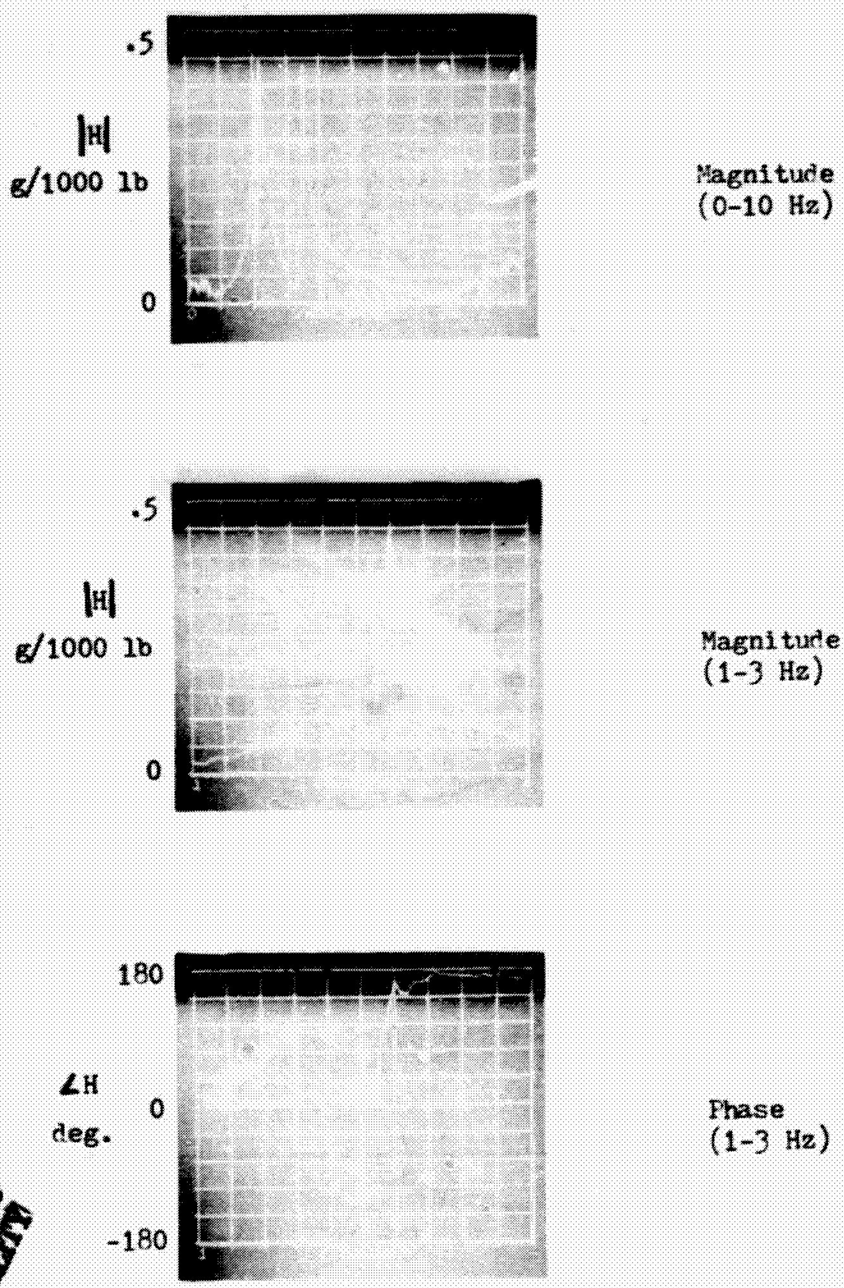

Figure 11. Details of two low frequency lateral modes; short struts, .5-9 Hz broadband excitation, lateral hub response. (Run 3, Point 7)

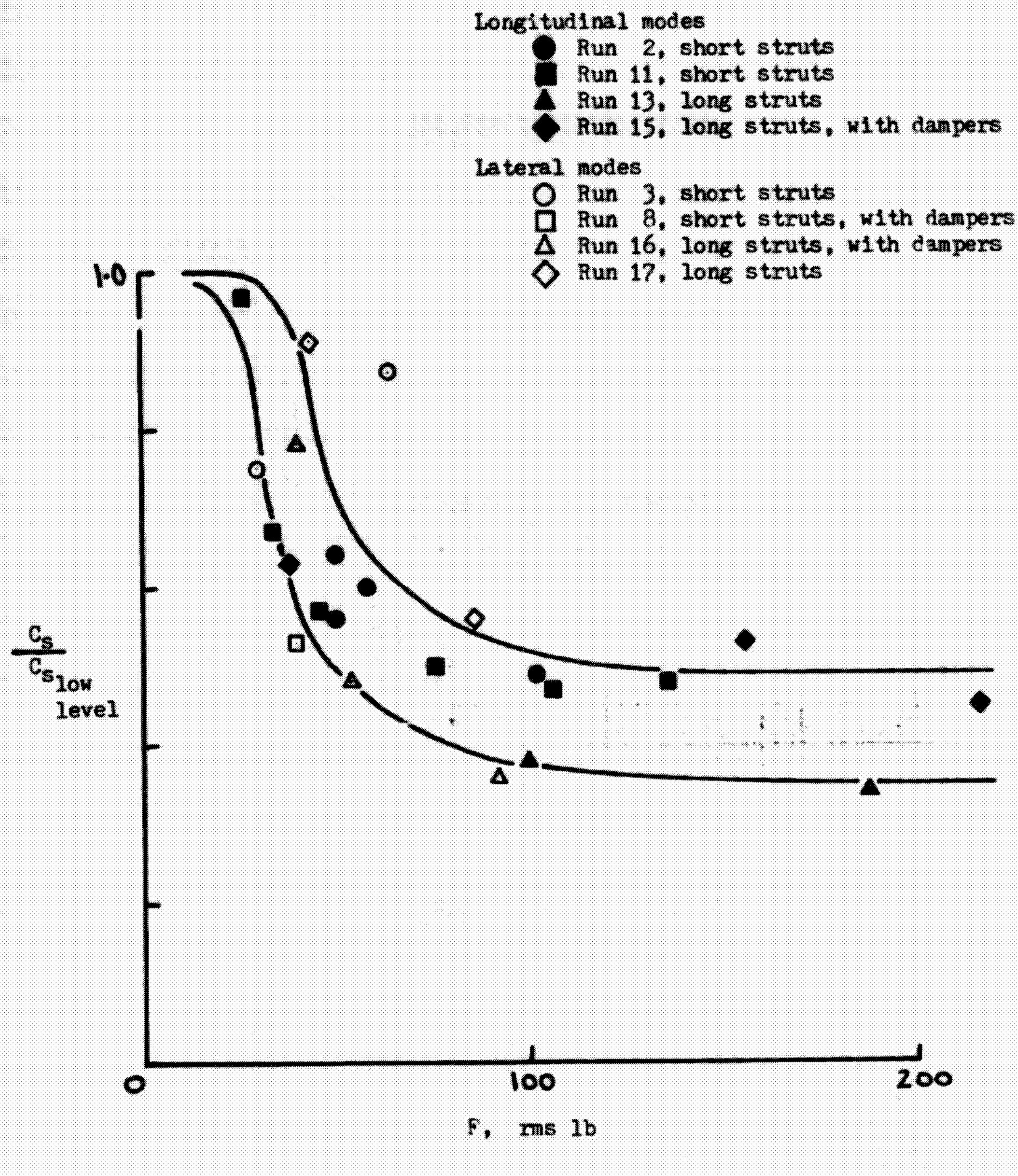

Figure 12. Nonlinear damping characteristics: reduction of fixed system damping (C_s) with excitation force level (F), for modes involving predominantly balance motion.